Mohammadi, Roozbeh; Roncoli, Claudio; Mladenovic, Milos

# Signalised intersection control in a connected vehicle environment: User throughput maximisation strategy

*Published in:*
IET Intelligent Transport Systems

*DOI:*
10.1049/itr2.12038

Published: 01/03/2021

*Document Version*
Publisher's PDF, also known as Version of record

Received: 9 September 2020 | Revised: 23 December 2020 | Accepted: 26 January 2021

IET Intelligent Transport Systems

DOI: 10.1049/itr2.12038

The Institution of Engineering and Technology WILEY

ORIGINAL RESEARCH PAPER

# Signalised intersection control in a connected vehicle environment: User throughput maximisation strategy

**Roozbeh Mohammadi** | **Claudio Roncoli** | **Miloš N. Mladenović**

Department of Built Environment, School of Engineering, Aalto University, Espoo, Finland

**Correspondence**
Roozbeh Mohammadi, Department of Built Environment, School of Engineering, Aalto University, Espoo 02150, Finland.
Email: roozbeh.mohammadi@aalto.fi

**Funding information**
FINEST Twins Center of Excellence (H2020 European Union funding for Research & Innovation grant 856602)

**Abstract**

Connected vehicle (CV) technology is expected to bring additional opportunities to share, collect, and exploit various information on vehicles and their occupants. Assuming that CVs are able to transmit on-board users and vehicle data, a user-based signal timing optimisation (UBSTO) strategy is proposed, designed to optimise user throughput for signalised intersections. In the CV environment, the inputs of the proposed algorithm consist of position and speed of CVs, as well as the number of passengers travelling in each vehicle, while the output is the optimum green time duration for each signal phase. In addition, authors' proposed strategy is able to adapt the cycle length to the traffic volume condition. In case of missing users data, the same strategy can also operate in vehicle-based mode, where the objective is vehicle-throughput maximization. The performance of the proposed strategy is compared with a fully actuated controller (FAC) in microscopic simulation, for several scenarios, including different CV penetration rates. Authors' findings show that UBSTO can effectively increase user throughput and decrease average user delay in comparison with FAC, while also prioritising vehicles with higher number of users on-board. These findings have implications for further development of prioritization strategies for public transport and ride-sharing vehicles.

## 1 | INTRODUCTION

Urban transport systems usually depend on traffic signal control for facilitating traffic flow and preventing extensive queuing and delays. Improving the performance of signalised intersections through development of management strategies relies on a range of detection mechanisms and control objectives [1–7]. The main detection mechanism in conventional traffic signal control consists dominantly of discrete point or area detection, using technologies such as inductive loops or video image processing [8–10]. These detection mechanisms are capable of providing data on various parameters, including vehicular flow and arrival speeds. Further development of detection and communication technologies have relied on the application of GPS, Bluetooth, RFID, and various other devices for special vehicle classes (e.g. emergency and transit vehicles) and intersections (e.g. grade-separated interchanges) [11–15].

Despite the technological advancements that have enabled diversification of control strategies, traffic control objectives have dominantly remained vehicle-centered, focusing on maximizing vehicular throughput or minimizing vehicular delay, stops, or queue lengths [16–19]. In contrast, some recent studies have focused more explicitly on passengers or persons in traffic operations problems. For example, Geroliminis et al. [20] suggested a three dimensional macroscopic fundamental diagrams based on passenger flow of cars and buses. Similarly, Chiabaut [21] introduced the concept of passenger macroscopic flow fundamental diagrams to develop a homogenized transportation network with different modes. In the field of traffic control, user-based performance measures are usually calculated as a side measure of vehicle-based indexes to evaluate the performance of a signal controller. For example, a classical approach for achieving this is by multiplying average occupancy factor of vehicles in existing vehicle delay models [22]. Following this, there is still a need to further develop and evaluate user-centered signal control strategies.

As one of the emerging technologies, Connected Vehicle (CV) is seen as a new major source of collecting reliable data

for various applications, including traffic management [23]. In particular, CVs allow collecting and processing high-resolution real-time data, which may be shared with the surrounding users, vehicles, and infrastructure [24]. Such data on flow volumes, travel times, queue lengths, and shock-wave boundaries originating from CV applications can be used in traffic signal control strategies [25–27]. In addition to vehicle data, CV technology may provide information on a range of user-related parameters. For instance, the number of users in each vehicle can be obtained through seat-belt activation or seat occupancy sensors, as opposed to estimating only average vehicle occupancy [28] or relying on resource-intensive efforts such as roadside windshield and the carousel method [29]. However, although CV data collection and communication capabilities may enable development of user-centred control strategies [30], such data have not been used to its full extent.

## 1.1 | Previous related research in traffic signal control

Improved detection and communication capabilities offered by CVs provide various opportunities for controlling signalised intersections, such as improved signal arterial coordination, public transport signal priority (PTSP), or signal-vehicle coupled control [24, 31–36]. User delay has been introduced as a metric in recent research regarding signal timing optimisation, mostly as a component for improved PTSP strategies in a multi-modal traffic environment. In fact, considering the number of passengers travelling on public transport vehicles and other modes helps to formulate PTSP problems that account also for non-public transport vehicles delay, which leads to clear advantages compared to conventional PTSP strategies such as preemption. In particular, Hu et al. proposed a controller to solve the problem of conflicting actuated-coordination and multi-modal priority, while priority-eligible modes such as public transport are equipped with V2I connection and passenger cars are detected by conventional loop detectors. The problem is formulated as a request-based mixed-integer linear program. The proposed controller can reduce bus delay and pedestrian delay by 24.9% and 14%, respectively, in high traffic volume. This work has been extended by proposing PTSP strategies based on CV technology, deploying green time re-allocation and bus-signal coordination for isolated an coordinated intersections. The problem is solved via an optimisation approach, minimising total person delay considering buses and passenger cars occupancy, while assuming fixed cycle time, constant traffic flow rate, and a maximum of one PTSP request per cycle [37–39]. Simulation experiments have shown that this approach can reduce bus delay between 55% and 75% compared to the conventional PTSP. Wu et al. [40] presented an integrated optimisation approach considering bus holding times at stops, signal timings, and bus speed recommendations to provide priority for buses at isolated intersections [41]. Simulation results indicate that the average bus delay can be reduced up to 24.2% by minimising the average vehicle delays, while ensuring that the bus clears the intersection without stopping at a red light. In order to address the limitation of the effective range of vehicle to infrastructure communications, a peer-to-peer priority signal control, solved using a mixed integer linear programming has been proposed in [42]. Yang et al. [43] developed a multi-modal PTSP strategy considering near-side and far-side bus stops and bus schedule delay to minimise bus and car delays. In a recent study, Wu et al. [44] investigated the effect of PTSP on moving bottleneck at signalised intersections in connected car and bus environment. Additionally, a real-time PTSP has been proposed by considering the migration states of coordinated phases and queuing states of non-public transport vehicles for the single-ring sequential phasing in [45]. A cooperative PTSP using vehicle to vehicle and vehicle to infrastructure communication has been also developed and investigated by Abdelhalim and Abbas [46], which could reduce 61% of public transport network delay compared to the base scenario. Moreover, a stream of works focused on the development of traffic signal control strategies for minimising person delay in conventional signal settings. Firstly, a real-time traffic-responsive signal control system with PTSP for an isolated intersection was proposed by Christofa et al. [47]. The aim of the developed controller was to determine signal settings in order to provide priority for public transport vehicles while minimising total person delay. Furthermore, the controller minimises adverse effect of PTSP on the passenger car delay by considering vehicles occupancy. This work was extended in [48, 49] by improving the mathematical formulation for unsaturated condition, adding further experimental scenarios, and considering other performance measures, such as number of stops and emissions. As a further step, Christofa et al. [50] extended the same framework to arterial conditions, considering multiple public transport lines traveling in conflicting directions and platooned vehicle arrivals. In addition, they introduced a weight factor to consider adherence of public transport vehicle to the schedule. This framework has been implemented in some subsequent studies for flexible cycle lengths [51], for phase rotation [52], and for evaluating public transport preferential treatments strategy [53]. Note that, in all these works, the underlying model predicts the delay for each of the lane groups and not for each individual vehicle, thus the total person delay was calculated by multiplying average vehicle occupancy by total delay. Hence, the method is not developed based on CV capabilities and is assumed to work with data from conventional sources such as inductive loop detectors, for all vehicles, and automated vehicle location systems for public transport vehicles.

Zeng et al. [54] considered individual vehicle occupancy in order to minimise the total person delay, assuming a CV environment with cars and buses. Two separate models for queuing vehicles and arriving vehicles were proposed, with the purpose of predicting the arrival time of each vehicle at the intersection and calculating delay. Considering average occupancy for each passenger car and bus, the proposed framework is able to reduced person delay up to 11% and bus delay up to 39% compared to SYNCHRO optimisation in undersaturated traffic condition. This model also showed decent performance in low CV penetration rate. However, the model performance was measured in undersaturated condition and using fixed signal cycle time. In another research, a passenger-based adaptive controller

was proposed [55]. The control mechanism extends the green time considering arrival time of vehicles, number of passengers, as well as pollution and fuel consumption. In addition to signal timing optimisation, concept of users has been considered to increase the capacity of intersection from passengers' perspective in [56] for the design of lane markings, exclusive bus lanes, and passive bus priority signal settings.

In conclusion, previous research mostly focuses on the following aspects. First, the focus is on the estimation of approach average delay considering average number of person per vehicle. Second, the focus is on the development of person-based strategies only to provide priority for public transport vehicles, without considering actual number of passengers on-board of passenger cars. Third, the focus is on the evaluation of controllers in specific traffic conditions, such as undersaturated traffic.

### 1.2 | Aims and contributions

This research relies on CV capabilities in data collection and transmission, which can easily obtain and communicate user-related information to a large number of sources in near real-time. Such technological capability is a cornerstone for developing the proposed user-based traffic control strategy. Other CVs capabilities, such as driving assistance technology and cooperation with other CVs, can improve signal controller performance [57, 58]. In this study, we focus on data transmission ability of CVs that can be used instead of conventional loop detectors or cameras. Consequently, we assume that CV behaviour does not differ from behaviour of manually-driven vehicles. This work extends the method presented in our previous work [59], as following:

- We include signal cycle dynamic adaptation to the controller, which allows to employ flexible cycle length while in the [59], the controller has been developed based on a fixed cycle time.
- We have considerably expanded the performance testing of the controller. First, we run the simulation in a mixed user demand combination where all type of vehicles are included in the flows arriving from all approaches of the intersection, whereas in [59], each vehicle type was assigned to a dedicated approach of the intersection. Second, we test the controller under three traffic flow conditions and five user demand combinations that lead to fifteen unique scenarios for each controller type. Third, the controller performance is compared to a fully actuated controller that was not included in the previous paper. Fourth, we also measure and compare other performance metrics, such as delay and number of stops, which were not measured in our previous work.
- We test the controller robustness in a partially CV environment, where the controller is no able to detect unequipped vehicles' data. This experimentation was not considered in the previous paper.

The main contributions of this paper can be summarised as follows. First, we propose a user-based signal time optimisation (UBSTO) strategy, aimed at finding the optimum signal timing that maximises user flow throughput within a signal cycle, as opposed to vehicular flow throughput. Second, the developed strategy accounts for known (measured or estimated) number of users on-board, as opposed to average occupancy rates. Third, the developed strategy relies on advanced CV capabilities, which allows an accurate prediction of users arrival time at the intersection, unlike previous works that are based on total (average) approach delay. Fourth, the developed strategy is also responsive to traffic demand through a flexible cycle length and is characterised by a reasonable computational time. Finally, the developed strategy is evaluated with simulation experiments in a wide range of different traffic conditions and various vehicle classes. Moreover, the robustness of the controller is tested in a partially CV environment under various penetration rates.

The remainder of this paper is organised as follows. Section 2 presents the formulation of the UBSTO strategy. Section 3 describes the implementation of UBSTO in a simulation experiment. Numerical results, in terms of model validation and control strategy evaluation, are presented in Section 4. Finally, Section 5 presents a summary and discussion of key findings, as well as and outline further research directions.

## 2 | METHODOLOGY FOR SIGNAL TIMING OPTIMISATION

The proposed UBSTO strategy consists of three main components. The first component consists of an analytical model predicting vehicle- and user-throughput within a signal control cycle; the second one formulates and solves an optimisation problem to find the optimum set of green times for signal control phases in order to maximise user-throughput; and the third one is an algorithm for re-adjusting green times and signal cycle based on predicted passage times, in order to further reduce delays. For controller design, we assume availability of vehicle data including speed, location, and length, similar to, for example, [60] and [4]. In addition, the number of users in each vehicle can be provided by on-board sensors such as seat-belt activation or seat occupancy sensors, and communicated via V2I. However, the proposed strategy proves to be efficient also in case of lower CV penetration rate, as it is demonstrated in our simulation experiments presented in Section 4.4. On the other hand, the required vehicle data can be estimated using information from a limited amount of CVs or can be collected by infrastructure-based traffic data collection methods; whereas, in case of missing information on the number of users, this can be replaced by average values based on historical data. A summary of the notation used throughout the paper is presented in Table 1. The remaining part of this section elaborates on the different components of the proposed strategy.

### 2.1 | User-throughput prediction

In order to calculate the user-throughput at an arbitrary intersection during a signal cycle, we develop first an algorithm

**TABLE 1** Notations

| Notation | Definition |
|---|---|
| $i$ | Signal phase index ($i = 1, 2, \dots, I$) |
| $j$ | Ring index ($j = 1, 2, \dots, J$) |
| $n$ | Vehicle index ($n = 1, 2, \dots, N_{ij}$), defined for each phase $i$ and ring $j$ |
| $\alpha_{ij}^n$ | Binary variable indicating if vehicle $n$ arrives at the stop-bar before ($\alpha_{ij}^n = 1$) or during ($\alpha_{ij}^n = 0$) green time |
| $\beta_{ij}^n$ | Binary variable indicating if vehicle $n$ will join the queue before discharging ($\beta_{ij}^n = 1$) or not ($\beta_{ij}^n = 0$) |
| $\gamma_{ij}^n$ | Estimated travel time for vehicle $n$ to reach the tail of the queue [s] |
| $\delta_{ij}^n$ | Time interval from when the backward recovery shock-wave reaches the tail of the queue to when the tail of queue passes the stop-bar for vehicle $n$ [s] |
| $\theta_{ij}^n$ | Time interval from the starting of cycle to when the backward recovery shock-wave reaches the tail of the queue for vehicle $n$ [s] |
| $\kappa$ | Threshold parameter for identifying queuing vehicles [m/s] |
| $\mu_{ij}^n$ | Travel time from updated position of vehicle $n$ to tail of moving queue [s] |
| $\phi_{ij}^n$ | Binary variable indicating if vehicle $n$ joins the queue while discharging ($\phi_{ij}^n = 1$) or it passes the stop-bar after the queue is discharged ($\phi_{ij}^n = 0$) |
| $c_{ij}$ | Time between the starting of cycle and the starting of phase $i$ in ring $j$ [s] |
| $C$ | Cycle time [s] |
| $d_{ij}^n$ | Initial distance between the head of vehicle $n$ and the stop-bar [m] |
| $D_{ij}^n$ | Updated position of vehicle $n$ when the backward recovery shock-wave arrives at the queue tail [m] |
| $g_{i,\min}$ | Minimum green time for phase $i$ [s] |
| $g_{i,\max}$ | Maximum green time for phase $i$ [s] |
| $G_i$ | End of green time for phase $i$ [s] |
| $g_i$ | Green time assigned to phase $i$ [s] |
| $\underline{g}$ | Set of all green times $g_i$ for all phases $i = 1, 2, \dots, I$ |
| $\Omega_i$ | Adapted green time of phase $i$ [s] |
| $s_i$ | Modified start of green time for phase $i$ [s] |
| $e_i$ | Modified end time of green for phase $i$ [s] |
| $\tau_i$ | Time from the starting of phase $i$ to when the last vehicle passes the stop-bar [s] |
| $H$ | Time headway between vehicles (and time gap between starting of green and the stop-bar passage of first vehicle) [s] |
| $L_{ij}^n$ | Length of vehicle $n$ in phase $i$ of ring $j$ [m] |
| $p_{ij}^n$ | Binary variable indicating if vehicle $n$ is served during current cycle ($p_{ij}^n = 1$) or not ($p_{ij}^n = 0$) |
| $Q_{ij}^n$ | Queue length when vehicle $n$ in lane assigned for phase $i$ in ring $j$ is being analysed [m] |
| $q_{ij}^n$ | Binary variable indicating if the vehicle $n$ is in queue ($q_{ij}^n = 1$) or not ($q_{ij}^n = 0$) |
| $S$ | Safety distance between stopped vehicles [m] |
| $t_{ij}^n$ | Travel time between the initial position of vehicle $n$ to the stop-bar in assigned lane for phase $i$ of ring $j$ [s] |
| $T_{ij}^n$ | Time from the starting of cycle to when vehicle $n$ in phase $i$ of ring $j$, passes the stop-bar [s] |
| $u_{ij}^n$ | Number of users in vehicle $n$ |
| $v_{ij}^n$ | Speed of vehicle $n$ in phase $i$ of ring $j$ [m/s] |
| $v_q$ | Vehicles speed in moving queue [m/s] |
| $v_s$ | Backward recovery shock-wave speed [m/s] |
| $Y$ | Amber and all red time duration [s] |

that, given the position and speed of vehicles approaching the intersection, as well as the sequence and duration of green times, predicts whether a vehicle can pass the stop-bar or not. We assume that vehicles in each approach are processed starting from the vehicle closest to the stop-bar ($n = 1$) to the last detected vehicle for a given detection area, defined, for example, in the range 200–1000 m. The comparison between the predicted stop-bar passage time for each vehicle and the remaining duration of green time determines if a vehicle will pass the stop-bar or not. The user-throughput calculation process is summarized in Algorithm 1 and detailed as follows.

### 2.1.1 | Vehicle passage condition

The comparison between the predicted vehicle arrival time and the end of green time for the corresponding phase determines if a vehicle crosses the intersection during the current cycle time in each of the approaches, which are processed simultaneously. This is calculated as

$$p_{ij}^n = \begin{cases} 1, & \text{if } T_{ij}^n < G_i \\ 0, & \text{otherwise,} \end{cases} \tag{1}$$

where

$$G_i = \sum_{i=1}^{I} g_i + (i-1)Y, \tag{2}$$

is the end of the green time for each phase $i$, assuming known phase sequence and green times assigned to each phase. We proceed then by elaborating on the computation of the predicted vehicle passage time $T_{ij}^n$.

### 2.1.2 | Vehicle passage time estimation

Some previous works suggested the classification of vehicles arriving at an intersection by considering a set of arrival conditions. For example, Feng et al. [61] proposed to categorise vehicles in three sets, namely (a) vehicles arriving to queuing region, (b) vehicles arriving in the slow-down region, and (c) vehicles travelling in the free-flow region; this classification was used in an adaptive signal control framework. Christofa et al. [50] proposed six cases for arriving platoons (for cars and buses) at an intersection, where the total delay is calculated for each

**ALGORITHM 1** User throughput calculation

**Input**: Location, speed, vehicle length and number of users for all connected vehicles within the detection area; phase sequence and green time duration for each phase during the next signal cycle
**Output**: User throughput for each approach during the next cycle time
**for** each approach of the intersection **do**
  **if** vehicle is not in queue (speed is higher than the threshold $\kappa$) **then** ▷ (Case 1)
    Calculate the arrival time of the vehicle to stop-bar based on (4)
    Compare it to beginning time of the green
    **if** vehicle arrival time is smaller than beginning time of the green **then** ▷ (Case 1.1)
      The vehicle arrives at the stop-bar before starting of green and it has to stop
      Calculate the arrival time of the vehicle at the stop-bar via (6) and update the queue length via (8)
    **else** ▷ (Case 1.2)
      The vehicle arrives at the stop-bar when signal is green
      Calculate the arrival time of the vehicle at the stop-bar based on (6)
    **end if**
  **else**
    Calculate the arrival time of the vehicle at the stop-bar via (11) and update the queue length via (12)
  **end if**
  **for** each other vehicle in the approach **do**
    **if** vehicle is in queue (speed smaller than $\kappa$) **then** ▷ (Case 2)
      Calculate the arrival time of the vehicle at the stop-bar via (11) and update the queue length via (12)
    **else**
      **if** There are not queuing vehicles at the stop-bar **then** ▷ (Case 3)
        Calculate the arrival time of the vehicle at the stop-bar via (4)
      **else**
        Compare the time the queue is starting to discharge (15) and the time when the vehicle reaches the end of the queue (14) using (13)
        **if** The start of queue discharging time is lower than the vehicle arrival time **then** ▷ (Case 3.1)
          Compare queue discharging time (19) and arrival time of vehicle to moving queue (Equations 17 and 18).
          **if** Vehicle reaches the queue during discharging **then** ▷ (Case 3.2)
            Compute the vehicle passage time via (22)
          **end if**
          **if** Vehicle cannot reach the queue during discharging **then**
            Compute the vehicle passage time via (24)
          **end if**
        **else** ▷ (Case 3.3)
          The vehicle joins the queue before discharging
          Compute the vehicle passage time via (20) and update the queue length via (21)
        **end if**
      **end if**
    **end if**
    **if** The vehicle stop-bar passage time is lower than remaining of the green time for the assigned phase **then**
      The vehicle passes the intersection in the current cycle
    **end if**
  **end for**
**end for**
Compute the user throughput by summing number of users on the vehicle passes the intersection

platoon of vehicles based on the arrival type. Authors of [54] proposed an algorithm treating every vehicle separately, leading to identical delay models for passenger car and bus. The authors divided arriving vehicles into three separate groups depending on whether a vehicle can pass the intersection in the current and next cycle times. However, some possible arrival types were not considered in such classification. Our prediction algorithm defines accurate arrival time to the stop-bar $T_{ij}^{n}$ for each vehicle separately, similarly to the work by Zeng et al. [54], while we consider comprehensive arriving patterns, similarly as in [50]. We do not consider stochastic nature of driving behaviour in the vehicle passage time estimation model. However, we validate the model accuracy, as shown in Section 4.1. In addition, we use different random seeds in our simulation experimentation, which considers the effect of stochastic driving behaviour on the controller performance. Thus, we do not increase computational time for estimation, while maintaining significant level of validity for intersection control purposes. We assume that, at the beginning of each cycle, updated data is available for all CVs present in the proximity of the intersection. Then, we classify arriving vehicles at each approach into three different main cases, which are further subdivided into six sub-cases. Then, based on each case properties, analytical methods for stop-bar passage time prediction are formulated. We first calculate the queue length based on the current vehicle information, which includes position, speed and length of the vehicle. Accordingly, our model takes into account the reported length of the arriving vehicles. As the decision of assigning each vehicle to each of developed cases is made at the beginning of each cycle, the decision making step size is equal to the cycle time. In our modeling approach we assume that, if the speed of a vehicle is smaller than a given threshold $\kappa$, the vehicle is in the queue. Accordingly, the queue length is defined as the distance between the head of the last stopped vehicle and the stop-bar. We assume that, once vehicles in queue starts moving, they all move with identical speed, constant safety distance, and constant time headway, similarly as in the [58, 61]. In addition, the desired speed for all vehicles is assumed constant and identical, which could be, for example, the speed limit of the road. For the vehicles not currently detected as in queue, the first criterion for classification is whether the vehicle will join the existing queue or not. Kinematic wave theory is used as main discriminant in this formulation [62], in addition to minimum time headway to satisfy car-following principles. Previous works usually calculated queue discharging rate based on a given saturation flow rate, for example, in the range of 1800–1900 veh/h, which leads to

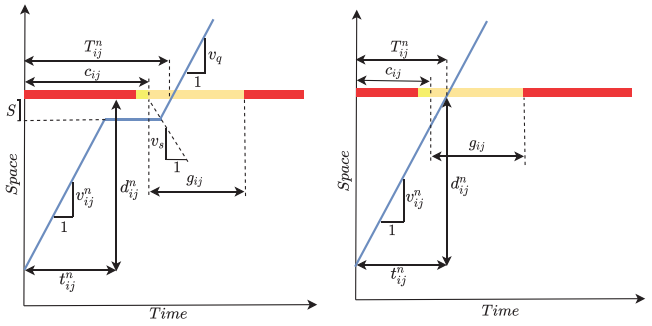


(a) Case 1.1 (b) Case 1.2

**FIGURE 1** Graphical representation of case 1

2 s time headway in queue discharging. However, recent studies showed that automated vehicles are able to move with lower headways, for example, 1 s and below [63]. In this regard, we use a precise formulation based on acceptable safety distance and time headway to calculate queue discharging speed and time, which allows to adjust the queue discharge rate based on the latest capabilities of CVs or the current situation, accounting, for example, for presence of automated vehicles. Overtaking is usually forbidden for vehicles approaching the intersection due to safety considerations [64]. Moreover, the possibility of lane changing may decrease in the future, as an increasing amount of vehicles are equipped with navigation system, which inform drivers on the lane to follow before entering into the intersection area[65]. Consequently, we do not consider lane changing and overtaking behaviour in the vehicle passage time estimation, whereas, any lane changes that may occur, act as (small) disturbances in our model. Similarly, [32, 61, 66] considered the same assumption about overtaking and lane changing in signalized intersection research. The developed cases for arrival vehicles are presented as follows.

- Case 1: Vehicle $n$ is the first moving vehicle
  In this case, the first detected vehicle is moving at a speed $v_{ij}^n > \kappa$. This case is further subdivided into two sub-cases based on whether the vehicle is predicted to arrive at the stop-bar before or during green time. Figure 1 shows a graphical representation of sub-cases of case 1. Blue and orange lines show trajectories of vehicle approaching the intersection and the vehicles already in queue, respectively. These sub-cases are identified by variable $\alpha_{ij}^n$, calculated as follows

$$\alpha_{ij}^n = \begin{cases} 1, & \text{if } t_{ij}^n < c_{ij}, \\ 0, & \text{otherwise}, \end{cases} \tag{3}$$

  where

$$t_{ij}^n = d_{ij}^n / v_{ij}^n, \tag{4}$$

$$c_{ij} = \sum_{k=1}^{i-1} g_k + (i-1)Y. \tag{5}$$

The travel time between vehicle position and the stop-bar is calculated by considering current vehicle speed (4), whereas a comparison between travel time and signal timing duration for the assigned phase determines the arrival conditions (3). For the vehicles assigned to the first phase, the travel time is compared with the assigned green time for the phase while for the other phases, the amber and red time duration before changing to green is also considered (5). Note that we assume each vehicle moves at a constant speed, equal to its current speed. Despite this assumption may affect the prediction accuracy as drivers may change their speed during the current cycle, we show later that, in a simulation experiment where this assumption is relaxed, there is no major impact on the prediction capabilities of this model. Case 1 is only defined for the first vehicle (closest to stop-bar) or for the next vehicles if the closest vehicles to the intersection can be served according to prediction. Depending on the resulting variable $\alpha_{ij}^n$, we further distinguish the following two sub-cases.

- Case 1.1: Vehicle $n$ is predicted to arrive at the stop-bar before the green time starts ($\alpha_{ij}^n = 1$)
  In this sub-case, vehicle $n$ is expected to stop at the safety distance before the stop-bar and wait until the green time starts. The arrival time to the stop-bar is calculated as follows

$$T_{ij}^n = c_{ij} + S\left(\frac{1}{v_q} + \frac{1}{v_s}\right), \tag{6}$$

  where

$$v_s = \left(\frac{H}{S} - \frac{1}{v_q}\right)^{-1}, \tag{7}$$

$$Q_{ij}^{n+1} = d_{ij}^n + L_{ij}^n. \tag{8}$$

  In addition to green duration in previous phases and the amber times, the stop-bar passage time also depends on the time gap between the start of green and when the vehicle starts moving, as well as the speed of vehicle. Regarding the latter, we assume that the speed of each vehicle in a moving queue $v_q$ is constant. In order to calculate the time gap between start of green and start of the vehicle movement, the backward recovery shockwave speed $v_s$ is used, assuming a constant time headway (7). Since vehicles stopping causes the queue to grow, the queue length needs to be updated for the next arriving vehicles, according to (8).
- Case 1.2: Vehicle $n$ is predicted to arrive at the stop-bar during green time ($\alpha_{ij}^n = 0$)
  In this case, vehicle $n$ arrives at the stop-bar during green time and is expected to pass the intersection without stopping. In this case, the queue length remains zero. Stop-bar passage time for vehicle $n$ is calculated as:

$$T_{ij}^n = t_{ij}^n, \tag{9}$$

$$Q_{ij}^{n+1} = 0. \tag{10}$$

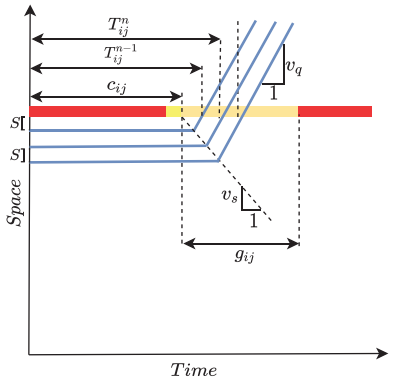


(a) Case 2

**FIGURE 2** Graphical representation of case 2

- Case 2: Vehicle $n$ is in queue
  In this case, vehicle $n$ has a speed $v_{ij}^n \leq \kappa$ and is expected to be served during the current green time as a part of the queue. While the first car in the queue is considered in a similar way as for Case 1.1, the stop-bar passage time for next vehicles is calculated based on the front vehicle passage time as follows:

$$T_{ij}^n = \begin{cases} c_{ij} + S\left(\frac{1}{v_q} + \frac{1}{v_s}\right), & \text{if } n = 1, \\ T_{ij}^{n-1} + \left(S + L_{ij}^{n-1}\right)\left(\frac{1}{v_q} + \frac{1}{v_s}\right), & \text{if } n > 1, \end{cases} \tag{11}$$

  while queue length does not increase, namely:

$$Q_{ij}^{n+1} = Q_{ij}^n. \tag{12}$$

  Figure 2 shows a graphical representation of sub-cases of case 2, where the blue line shows trajectories of vehicles approaching the intersection.
- Case 3: Vehicle $n$ is approaching the intersection while there is a queue
  In this case, vehicle $n$ moves towards the intersection approaching an existing queue. We define three sub-cases depending on whether vehicle $n$ is predicted to reach the tail of the queue before clearance, during clearance, or pass the intersection after queue clearance. To determine if vehicle $n$ will reach the tail of the queue before clearance, we calculate variable $\beta_{ij}^n$ as follows

$$\beta_{ij}^n = \begin{cases} 1, & \text{if } \gamma_{ij}^n < \theta_{ij}^n, \\ 0, & \text{otherwise,} \end{cases} \tag{13}$$

  where

$$\gamma_{ij}^n = \frac{d_{ij}^n - (Q_{ij}^n + S)}{v_{ij}}, \tag{14}$$

$$\theta_{ij}^n = c_{ij} + \frac{Q_{ij}^n}{v_s}. \tag{15}$$

  Travel time between vehicle position and tail of queue (considering a safety distance) is calculated via (14), whereas (15) determines the queue clearance time. Then, by comparing the vehicle travel time and queue clearance time, we can determine if the vehicle arrives at the queue tail before starting of clearance or not.
  If the previous calculation predicts that vehicle $n$ cannot join the queue before the queue starts to discharge, that is, $\beta_{ij}^n = 0$, a second level of classification is performed to determine if the vehicle joins the queue during discharge or it passes the stop-bar after the queue has discharged, which is described by $\phi_{ij}^n$, calculated as follows.

$$\phi_{ij}^n = \begin{cases} 1, & \text{if } \delta_{ij}^n > \mu_{ij}^n, \\ 0, & \text{otherwise,} \end{cases} \tag{16}$$

  where

$$D_{ij}^n = d_{ij}^n - v_{ij}^n \frac{Q_{ij}^n}{v_s}, \tag{17}$$

$$\mu_{ij}^n = \frac{D_{ij}^n - Q_{ij}^n}{v_{ij}^n - v_q}, \tag{18}$$

$$\delta_{ij}^n = \frac{Q_{ij}^n}{v_q}. \tag{19}$$

  Equation (17) determines updated distance of vehicle $n$ to the stop-bar at the time that the queue starts discharging. Then, we calculate queue discharging time and the time required for vehicle $n$ to reach the queue tail (18), (19). Depending on the variables $\beta_{ij}^n$ and $\phi_{ij}^n$, the following sub-cases are defined.
  - Case 3.1: Vehicle $n$ arrives at the tail of the queue before queue starts to discharge ($\beta_{ij}^n = 1$)
    As the vehicle joins the queue, stop-bar passage time in this condition is calculated based on previous vehicle calculated stop-bar passage time ($T_{ij}^{n-1}$), backward recovery shock-wave, and queue discharging speed. Since the vehicle is predicted to join the queue, its length should be updated.

$$T_{ij}^n = T_{ij}^{n-1} + (S + L_{ij}^{n-1}\left(\frac{1}{v_q} + \frac{1}{v_s}\right), \tag{20}$$

$$Q_{ij}^{n+1} = Q_{ij}^n + l_{ij}^n + S. \tag{21}$$

  - Case 3.2: Vehicle $n$ arrives at the tail of the queue during queue discharging ($\beta_{ij}^n = 0$ and $\phi_{ij}^n = 1$)
    Similar to Case 3.1, the vehicle joins the queue; however, in this case, the queue is moving, thus backward recovery

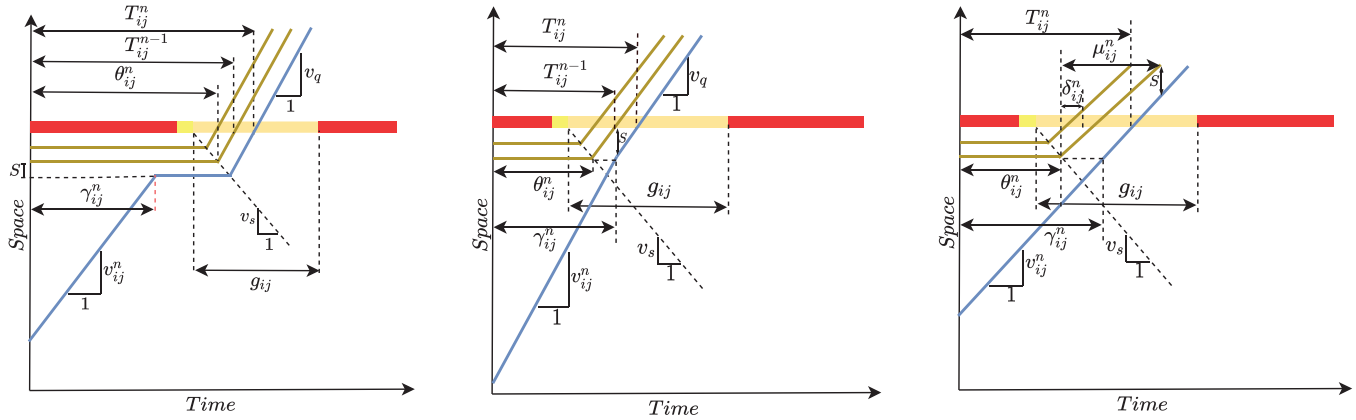


(a) Case 3.1 (b) Case 3.2 (c) Case 3.3

**FIGURE 3** Graphical representation of case 3

shock-wave speed is not considered. Moreover, the queue length is not expected to change.

$$T_{ij}^n = T_{ij}^{n-1} + \frac{S + L_{ij}^{n-1}}{v_q}, \tag{22}$$

$$Q_{ij}^{n+1} = Q_{ij}^n. \tag{23}$$

- Case 3.3: Vehicle $n$ cannot reach to tail of queue before or during discharge ($\beta_{ij}^n = 0$ and $\phi_{ij}^n = 0$)
  In this case, vehicle $n$ does not join the queue and passes the stop-bar after queue is completely discharged. Accordingly, queue length does not change.

$$T_{ij}^n = \frac{d_{ij}^n}{v_{ij}}, \tag{24}$$

$$Q_{ij}^{n+1} = Q_{ij}^n. \tag{25}$$

Figure 3 shows a graphical representation of sub-cases of case 3, where the blue and orange lines show trajectories of vehicle approaching the intersection and the vehicles already in queue, respectively.

## 2.2 | Signal timing optimisation

In this section, we present a method to compute the optimum set of green times for each phase in order to maximise the number of served users (or vehicles) in a cycle time, based on the prediction algorithm described in Section 2.1. Our optimisation problem is formulated in order to maximise user- (or vehicle-) throughput. Note however that, as we calculate the accurate arrival time for each vehicle, the same optimisation framework can be utilised to optimise different disaggregated performance metrics, for example, user (or vehicle) delay. In the following sections, we describe in detail the optimisation problem formulation and solution algorithm.

### 2.2.1 | Optimisation problem formulation

We formulate the following optimisation problem

$$\max_{\underline{g}} \sum_{j=1}^{J} \sum_{i=1}^{I} \sum_{n=1}^{N_{ij}} u_{ij}^n \, p_{ij}^n(\underline{g}), \tag{26}$$

subject to:

$$\sum_{i=1}^{I} g_i + (I-1)Y \leq C, \tag{27}$$

$$g_i \geqslant g_{i,\min} \quad \forall i, \tag{28}$$

$$g_i \leqslant g_{i,\max} \quad \forall i. \tag{29}$$

The objective function (26) consists of the total users throughput during the next cycle time, which is calculated based on the prediction of vehicles that are served in a given green time set $p_{ij}^n(\underline{g})$ and the (known) number of users in each vehicle $u_{ij}^n$. Note that $p_{ij}^n(\underline{g})$ is computed according to (1)–(25). We consider as constraints a maximum cycle time (27) and lower- and upper-bounds for the green times in each phase (28), (29). Note that, this optimisation problem can also be employed to maximise vehicle throughput instead of user throughput, by setting $u_{ij}^n = 1$ for all vehicles approaching the intersection.

### 2.2.2 | Solution method

The problem (26)–(29) is a mixed-integer nonlinear program (MINLP). In fact, the possibility of different user and vehicle

arrival patterns leads to a complex problem characterised by a large non-convex solution region. Consequently, solving this optimisation problem by analytical methods would lead to considerably high computation time—if we assume the problem is solvable—which is not acceptable for real time applications. For this reason, we employ a meta-heuristic algorithm, based on genetic algorithm (GA) method, which can find the nearly optimal solution by evaluating different sets of green times [67, 68]. At the beginning of each cycle, CV data are collected and converted into chromosomes and genes, in order to be processed by the GA solver. In particular, each chromosome represents a set of green times, where each gene corresponds to a phase of the traffic signal. Chromosomes are initialised via a random number generated based on minimum and maximum allowed green time. The fitness function of each chromosome is set equal to the cost of our optimisation problem (26), that is, the user throughput at the intersection, and is computed via the algorithm presented above. The throughput computation is done simultaneously for each chromosome by GA. Moreover, to avoid local optima, we run GA instances with different initial conditions. Note that most of these calculations can be implemented in a parallel fashion, allowing to obtain the solution in very reasonable computation times.

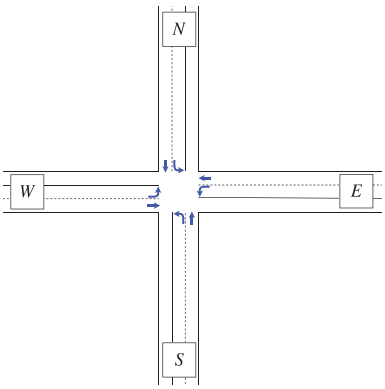


(a) Case intersection

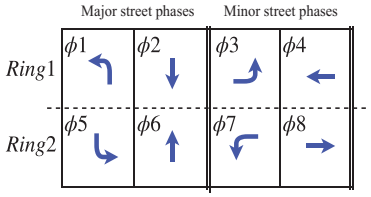


(b) Signal phasing diagram

**FIGURE 4** Simulation environment and signal settings

## 2.3 | Signal cycle dynamic adaptation

As mentioned previously, we consider the maximum cycle time as an upper-bound while searching for the optimum green time for each phase. However, as we use a heuristic solution method, which may lead to sub-optimal results due to the fact that the entire feasible solution space is not explored and the objective function of the problem is throughput (not delay), there is possibility of assigning unnecessary high green time to a phase just to satisfy the problem constraints. This is expected to happen higher frequently in low traffic flow conditions, where the last detected vehicle may pass the intersection a significant amount of time before the end of assigned green time. Hence, we designed a module for cycle adaptation in order to trim the excess green time at the end of each phase, which may be activated after the optimum set of green times is obtained via the GA algorithm. In other words, for each phase, we reduce the end of green time, calculated via our optimisation algorithm, by setting it equal to the passage time of the last detected vehicle, namely removing the green time during which no vehicles are predicted to reach the stop line. The adapted green time is calculated as follows:

$$\Omega_i = \max\left(e_i - s_i + 1, g_{i,\min}\right), \tag{30}$$

where

$$s_i = \begin{cases} 0, & \text{if } i = 1, \\ e_{i-1} + Y, & \text{if } i > 1, \end{cases} \tag{31}$$

$$e_i = \begin{cases} \tau_i, & \text{if } i = 1, \\ s_i + \tau_i, & \text{if } i > 1, \end{cases} \tag{32}$$

$$\tau_i = \begin{cases} \max(T_{i1}^N, T_{i2}^N, \dots, T_{ij}^N), & \text{if } i = 1 \\ \max(T_{i1}^N, T_{i2}^N, \dots, T_{ij}^N) - (g_{i-1} + (i-1)Y), & \text{if } i > 1 \end{cases}. \tag{33}$$

The passage time of the last served vehicle in each phase ($\tau_i$) is calculated considering the last served vehicle in each approach, denoted as $T_{ij}^N$. The start time of each phase is equal to the sum of end time of the previous phase and the transition phase length (amber and all red time) except first phase which starts at origin of time (31); while the end time for each phase is calculated based on (32), where $\tau_i$ is added to the start time of each phase, except from the first phase where the end time is equal to $\tau_i$. Note that we impose that $\Omega_i$ cannot be smaller than the minimum green time.

# 3 | SIMULATION SETUP

We test the performance of the proposed strategy via a set of simulation-based experiments. For this purpose, an artificial four-leg intersection, shown in Figure 4(a), is considered as test platform. Phase sequence settings are assumed according to NEMA standard ring-and-barrier as in Figure 4(b) [69]. We consider northbound and southbound as major approaches and eastbound and westbound as minor approaches. The traffic volume of minor through approaches is considered half of major through approaches, while left-turn traffic volumes are 0.25% of the through approach volumes. We test the performance of the strategy for two traffic demand levels, namely, (a) low demand, where the traffic demand is set half of the intersection nominal

capacity, that is, 1800 veh/h, and (b) high demand, where the traffic demand is close to saturation, that is, 3500 veh/h. Four type of vehicles, based on their number of users on board, are considered in traffic flow, denoted as U1, U2, U3, U4, where the number of users on-board is 1, 2, 3, and 4, respectively. Considering diverse combinations of vehicle classes, we simulate the intersection for five user demand combinations, which are presented in Table 2. In the first combination, vehicles with low number of user are assigned to major approaches while vehicles with high number of users are assigned to minor approaches: this implies that approaches with high-flow and few-users are directly competing versus approaches with low-flow and many-users. This relation is gradually changed from combination 1 to combination 5. The lowest average number of users per vehicle is 1.7 users per vehicle, which is close to the current real world averages [70]. The average user per vehicle for the maximum user demand combination is 3.3 users per vehicle. Combining the two vehicle demand levels and the five user demand combinations results in ten scenarios that we investigate in our simulations. While presenting the results, we denote scenarios as follows: a letter denotes the demand level, that is, L for low traffic demand and H for high traffic demand; while a number denotes the user demand combination, according to Table 2. For example, L-3 refers to the scenario with low traffic demand and user demand combination 3. The maximum green time is set as 60 s for all approaches and the minimum green time for through and left turn approaches are 10 s and 5 s, respectively. Note that considering minimum green time is necessary to serve unequipped vehicles in the case of low penetration rate of connected vehicles, whereas, in a fully connected environment or by assuming presence of point data collection, such as loop detector, at the intersection, the controller can operate without considering any minimum green time. The maximum cycle time is considered 60 s and 120 s for low and high traffic demand, respectively.

We employ the microscopic simulation software VISSIM [71] as traffic simulation platform and MATLAB as programming software to implement our proposed methods and algorithms, while the interaction between VISSIM and MATLAB is implemented via COM interface. In order to reproduce stochastic nature of driving behaviour in traffic simulation, we utilise Wiedemann-74 car following model, while the parameters for each vehicles are stochastically sampled from random distributions. Each simulation scenario is run for one hour, while we consider 20 unique random seeds in order to account for stochastic users and vehicles arrival patterns. After a warm-up time of 2 min, data are collected from VISSIM at the beginning of each cycle and sent to the optimisation algorithm that iteratively computes the optimal set of green times; then, if active, these are the post-processed by the signal cycle dynamic adaptation algorithm. The set of green times is then returned to VISSIM that implements them as a the signal plan. A set of performance measures are collected in order to evaluate the strategy efficiency. Note that simulations are run in 20 unique random seeds to consider randomness of vehicle stochastic arrival pattern and stochastic nature of driving behaviour. Finally, we report average performance of the all random seeds for each scenario. Figure 5 details the simulation framework setup.

In order to reduce the risk of falling in local optima, every time we solve our optimisation problem, we run 10 separate instances of the GA, with random initial solutions, while the final green time split is selected as the best solution among those 10, that is, the solution with best fitness function value. In our experiments, we set a population size of 30 chromosomes and the GA is iterated for up to 40 generations. The computation time to find a optimum green is approximately 0.7 s using a laptop computer with a 4-core 3.4-GHz central processing unit. Note that, since GA instances can be run in a parallel fashion, total calculation time is not affected by running multiple instances.

We present numerical experiments to assess and evaluate the effectiveness of our proposed signal control strategy by comparing it with a state-of-the-art fully-actuated signal control strategy (FAC), as well as with a vehicle-based signal time optimisation (VBSTO) version of our optimisation method. The chosen FAC is a ring barrier controller [72], which is readily available in VISSIM, and it assumes the presence of vehicle detectors for all phases. Signal settings for FAC are the same as for UBSTO except for the maximum green time for each phase, which is computed by the tool VISTRO [73]. The VBSTO strategy is implemented and solved by the same algorithm as UBSTO, with the difference of considering vehicle throughput maximisation as objective, which is achieved by setting one user for each vehicle, that is, $u_{ij}^{n} = 1$ in (26). In addition to validation of user throughput prediction module, the evaluation of the proposed strategy focuses on the following performance measures: Difference in user throughput per approach for UBSTO, VBSTO, and FAC; Difference in average user delay per approach for UBSTO, VBST, and FAC; Average delay of different vehicle classes for UBSTO, VBSTO, and FAC; Difference in user throughput per CV penetration rate for UBSTO

**TABLE 2** User demand combinations used in the simulation experiments

| User demand combination | Major approach | | | | Average users per vehicle | Minor approach | | | | Average users per vehicle |
|---|---|---|---|---|---|---|---|---|---|---|
| | U1 | U2 | U3 | U4 | | U1 | U2 | U3 | U4 | |
| 1 | 45% | 45% | 5% | 5% | 1.7 | 5% | 5% | 45% | 45% | 3.3 |
| 2 | 30% | 30% | 20% | 20% | 2.3 | 20% | 20% | 30% | 30% | 2.7 |
| 3 | 25% | 25% | 25% | 25% | 2.5 | 25% | 25% | 25% | 25% | 2.5 |
| 4 | 20% | 20% | 30% | 30% | 2.7 | 30% | 30% | 20% | 20% | 2.3 |
| 5 | 5% | 5% | 45% | 45% | 3.3 | 45% | 45% | 5% | 5% | 1.7 |

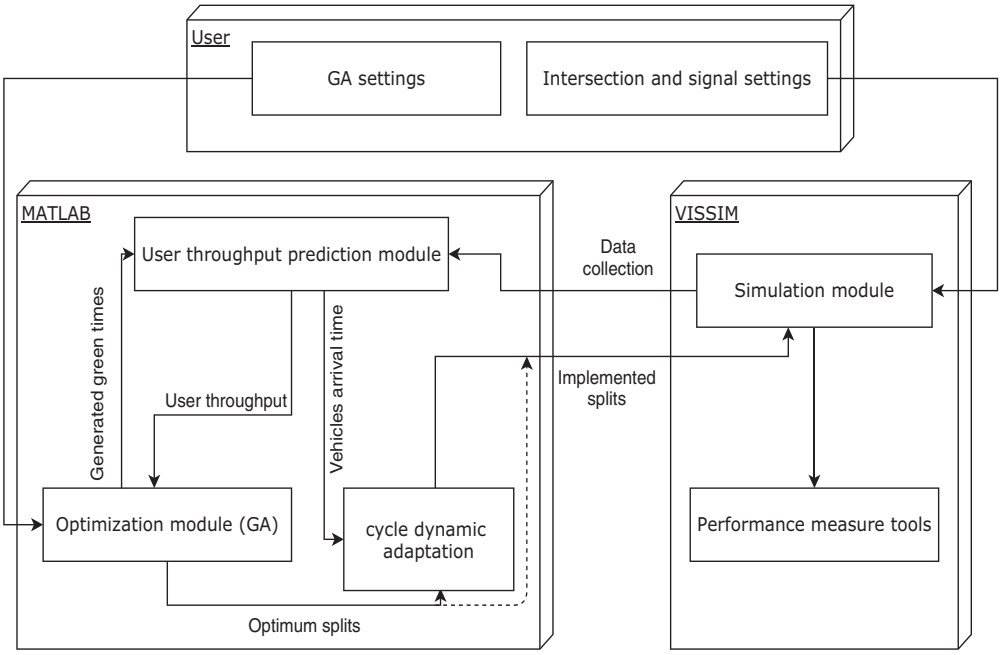


**FIGURE 5** Simulation framework setup

and FAC; Difference in average user delay per CV penetration rate for UBSTO and FAC; Average number of stops per vehicle per CV penetration rate for UBSTO and FAC; Difference in user throughput for UBSTO without cycle adaptation, UBSTO with cycle adaptation, and FAC; Difference in average user delay for UBSTO without cycle adaptation, UBSTO with cycle adaptation, and FAC.

## 4 | RESULTS OF SIMULATION EXPERIMENTS

### 4.1 | Validation of the user-throughput prediction model

Before proceeding with results involving signal timing optimisation, we present here a validation test designed in order to illustrate the accuracy of the proposed prediction model. In particular, we compare the accumulated user-throughput predicted by our model with the user-throughput measured in VISSIM, for two scenarios characterised by low and high traffic demand. The parameters used in our prediction algorithm are calibrated from data simulated by VISSIM and set as follows. The maximum allowed speed of the vehicles $v_d$ and queue discharging speed $v_q$ are set to 60 km/h and 20 km/h, respectively. Safety distance between vehicles ($S$) is set to 2 m and time headway ($H$) is set to 2 s. In case CVs are also automated, lower safety distance and time headway may be considered (see, e.g. [63]). Figure 6 shows result of algorithm validation for a ring within a cycle, where vertical red bars show the end of green time for each phase. Note that, the car-following model used in VISSIM accounts for stochastic features that reflect the nature of driving behaviour, which leads to somehow realistic results, but is also characterised by a large number of parameters that need to be calibrated. On the other hand, our prediction model considers well-defined simplifications of drivers' behaviours and requires a small set of parameters. Yet, we can see from our experiments that our models shows an acceptable accuracy in term of prediction of vehicles and users stop-bar passage time, that is, the difference between measured and predicted user throughput never exceeds 5 users in the considered cycle for both traffic condition. Moreover, although VISSIM uses a stochastic driving behaviour model, the prediction accuracy of our model is not affected significantly.

### 4.2 | Comparison of average user throughput and delay

In order to illustrate the benefits of the proposed strategy, we present here a series of simulation results, by comparing UBSTO with two other strategies, namely FAC and VBSTO. Firstly, we look into total user throughput and average user delay for UBSTO and VBSTO compared to FAC. Numerical results are presented in Figure 7 and Figure 8, respectively. In particular, we compare UBSTO and VBSTO performance effect on the throughput and average user delay of each approach of the intersection separately, as well as for the entire intersection. In low traffic demand, the improvement in serving users by employing UBSTO and VBSTO is demonstrated by smaller differences as compared to the ones in the high traffic demand. Moreover, by comparing UBSTO with VBSTO, we can observe the tendency of UBSTO to prioritise users rather than vehicles, as in most conditions UBSTO can serve more users than VBSTO.

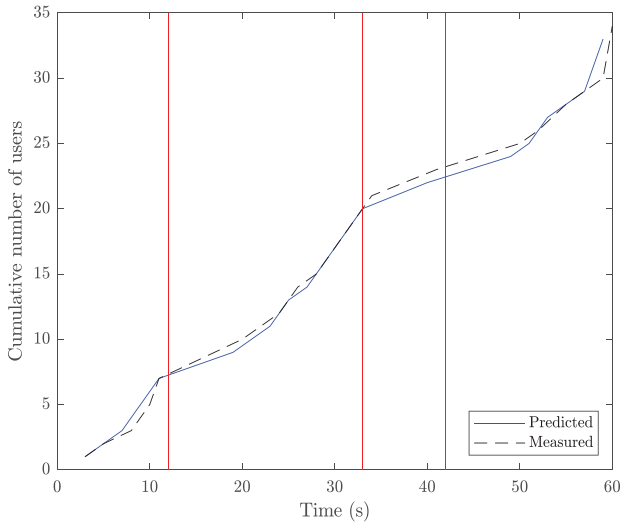


(a) Low vehicle flow

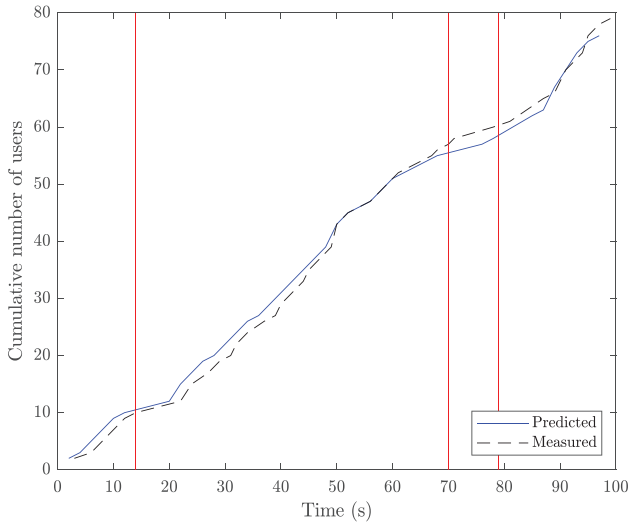


(b) High vehicle flow

**FIGURE 6** Validation of user throughput prediction

However, VBSTO outperforms UBSTO in some high demand scenarios, such as H-1 and H-2. Evaluating throughput per-approach reveals that UBSTO provides priority by serving more high occupancy vehicles, that is, in scenarios H-1 and H-2 where there are higher U3 and U4 vehicles in through-minor approach. This leads throughput increase for approaches with higher vehicle occupancy, which may contrast with the whole intersection throughput. Further details on the effect of UBSTO and VBSTO on each vehicle class performance are presented in Section 4.3.

In addition to the findings about throughput above, Figure 8 reveals that both UBSTO and VBSTO outperform FAC for all user demand combinations, considering the average user delay for the whole intersection. However, several cells with positive values (delay for FAC strategy is lower) can be seen in the user delay for through-minor approaches. For example, in the low traffic demand, the delay in through-minor approach by employing UBSTO and VBSTO is higher than by using FAC, while the total delay of the intersection is higher in the FAC case. Moreover, the change in through-major approach is smaller than left-turn on the major approach: this difference is attributed to the opposite concept of FAC and our proposed strategies. In fact, FAC serves vehicles based on detector actuation, therefore longer green time is provided for major approaches, while lower green time is assigned to left turns, due to difference in vehicular volume. On the contrary, UBSTO and VBSTO predict arrival time of each vehicle in the major or minor approach for the next cycle. Consequently, the controller considers all vehicles on the approaches, and not only the vehicle at point/area detectors. This leads to smaller reduction in major approaches delay compared to left turn lanes. Additionally, this causes higher delay in major approaches such as through-minor lanes in low traffic demand and through minor approaches in scenario H-5.

## 4.3 | Impact on different vehicle classes

Since UBSTO takes explicitly into account the number of users for each vehicle, we evaluate the influence of UBSTO on different vehicle classes, and compare results with vehicle-based controllers, by measuring the average delay for each vehicle class, as well as for all vehicles in low and high traffic conditions for three user demand combinations: 1, 3, and 5. This is illustrated in Figures 9 and 10, where we notice that for all the tested combinations, both UBSTO and VBSTO outperform FAC in terms of total vehicle delay. As expected, when using VBSTO as the control strategy, the average delay for all vehicles is smaller than or equal to UBSTO for all scenarios; this is due to the fact that VBSTO aims explicitly at maximising vehicle throughput. Additionally, the tendency of UBSTO to serve vehicles with higher number of users on-board leads to the lowest average delay for U3 and U4 compared to other controllers. However, the average delay for each vehicle class is sensitive to the user demand combinations. When the user arrival flows are equal in the major and minor approaches, the resulting vehicle classes delay are also similar when using UBSTO and VBSTO, since, basically, the objectives of the two controllers are aligned. Within scenario L-1, U3 and U4 delay by the three controllers are approximately the same, while the delay of U1 and U2 are considerably lower by UBSTO and VBSTO compared to FAC, which leads to lower delay for all vehicles while applying UBSTO and VBSTO. In high traffic scenarios with the same user demand combinations (scenario H-1), UBSTO causes higher delay for U1 and U2, as they are low occupancy vehicles, and considerably smaller delay for U3 and U4, as they are high occupancy vehicles. The same situation occurs in scenario H-5, where the possibility of serving higher number of U3 and U4 from major approaches results in even higher delay for U1 and U2 compared to FAC. Moreover, we tracked individual vehicles delay under each evaluated strategy for a single replication. In particular, in Figures 11 and 12, we present histogram plots showing the number of vehicles that experience different delay values, grouped in bins of

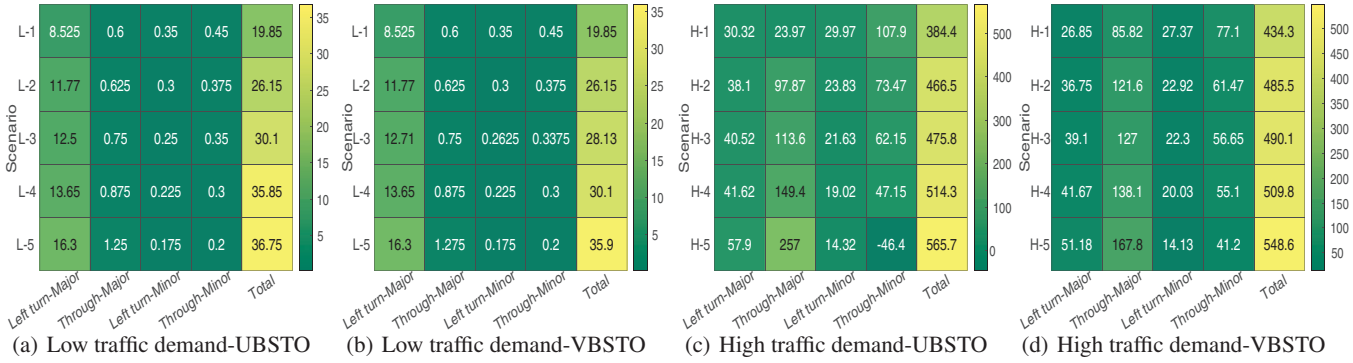


(a) Low traffic demand-UBSTO (b) Low traffic demand-VBSTO (c) High traffic demand-UBSTO (d) High traffic demand-VBSTO

**FIGURE 7** Difference in user throughput between UBSTO and FAC (a,c) and between VBSTO and FAC (b,d)

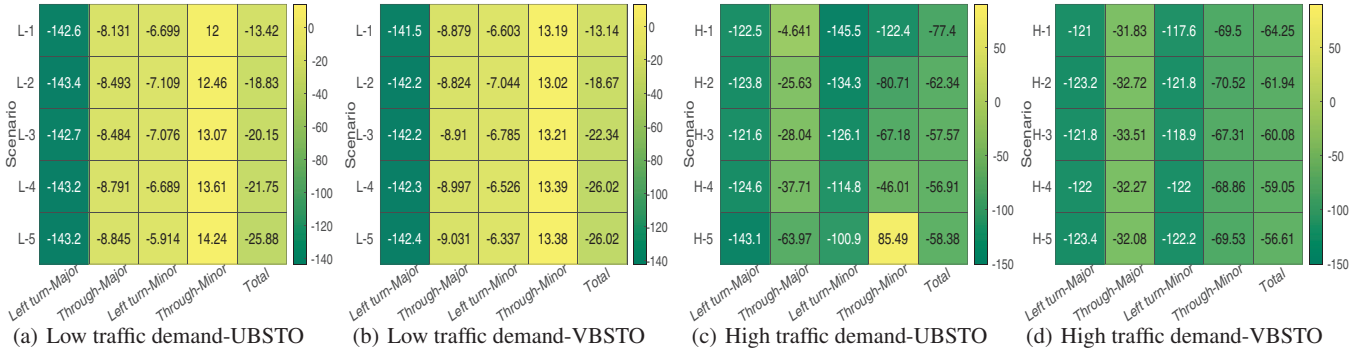


(a) Low traffic demand-UBSTO (b) Low traffic demand-VBSTO (c) High traffic demand-UBSTO (d) High traffic demand-VBSTO

**FIGURE 8** Difference in average user delay (s) between UBSTO and FAC (a,c) and between VBSTO and FAC (b,d)

10 s considering scenarios H1 and H5. Note that, for the sake of brevity, we present only U1 and U4 as representative of low and high occupancy vehicles. The maximum delay for individual vehicles is considerably higher while employing FAC compared to UBSTO and VBSTO. For example, the maximum delay in H-1 with FAC is close to 1000 s, while the delay does not exceed 300 s in UBSTO and VBSTO. Figures 11(a) and 12(a) illustrate that UBSTO maximises the user throughput by serving higher amount of high occupancy vehicles. In H-1, where the U4 are in minor approaches and U1 in major approaches, UBSTO leads to delays of the same magnitude; whereas, in H-5, where the U4 are in major approaches and U1 in minor approaches, delays for U4 are considerably lower than for U1. On the other hand, Figure 11(b) and Figure 12(b) show that VBSTO maintains similar values of vehicle delays for classes U1 and U4, as the control objective is to maximise vehicle throughput irrespectively of the users number. Additionally, the maximum frequency point of histograms are approximately in the same position for both U1

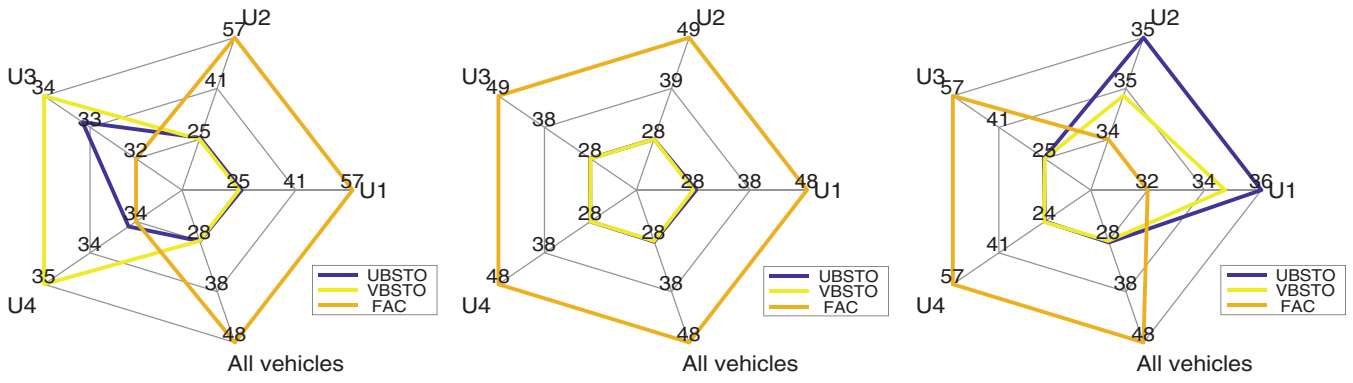


(a) L-1 (b) L-3 (c) L-5

**FIGURE 9** Comparison of the average delay (s) of different vehicle classes by UBSTO, VBSTO and FAC controller in low traffic demand

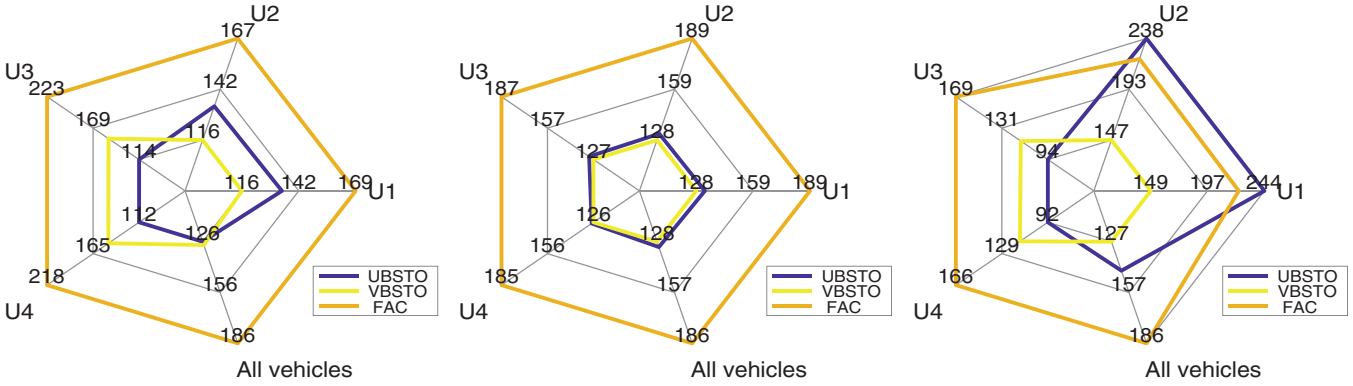


(a) H-1 (b) H-3 (c) H-5

**FIGURE 10** Comparison of the average delay (s) of different vehicle classes by UBSTO, VBSTO and FAC controller in high traffic demand

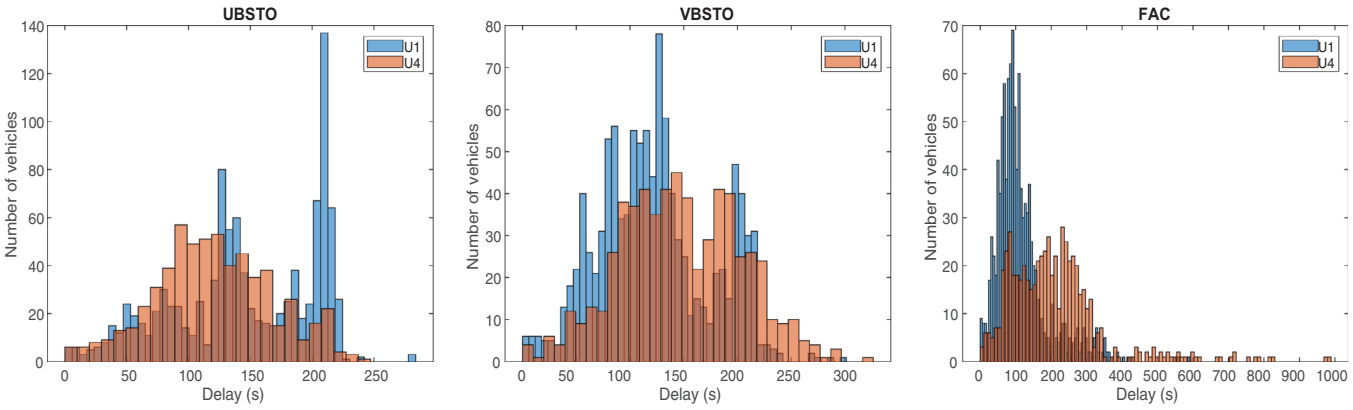


(a) H-1 - UBSTO (b) H-1 - VBSTO (c) H-1 - FAC

**FIGURE 11** Histograms of the U1 and U4 vehicle class delay in H-1 scenario by employing UBSTO, VBSTO, and FAC

and U4. As expected, FAC serves vehicles based only on overall flow in each approach, which leads to lower delay for vehicles in major approaches with high traffic flow. Accordingly, this leads to a lower delay for U1 in H-1 and a lower delay of U4 in H-5.

## 4.4 | Impact under different CV penetration rates

As previously stated, the prediction model employed in UBSTO takes as input speed and position of all the vehicles approaching

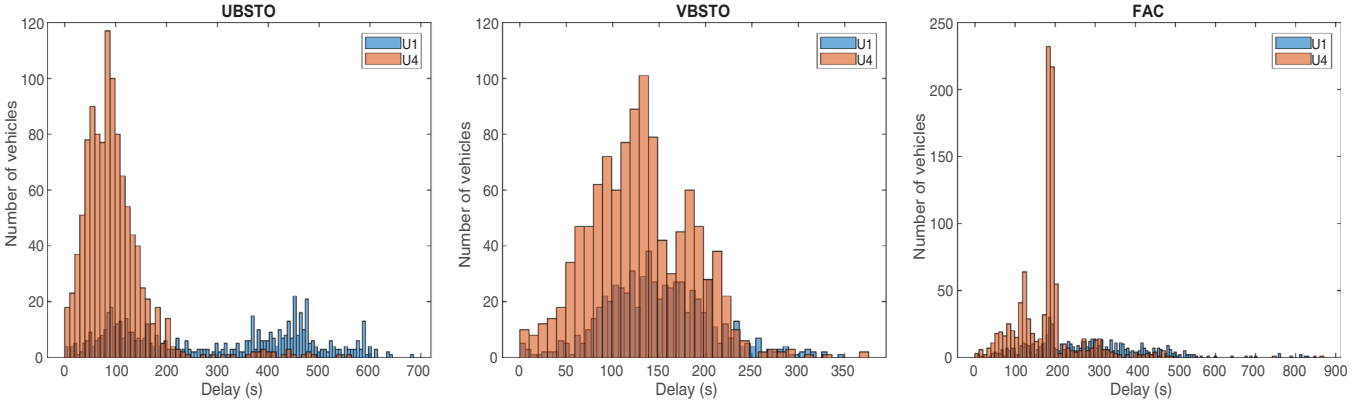


(a) H-5 - UBSTO (b) H-5 - VBSTO (c) H-5- FAC

**FIGURE 12** Histograms of the U1 and U4 vehicle class delay in H-5 scenario by employing UBSTO, VBSTO, and FAC

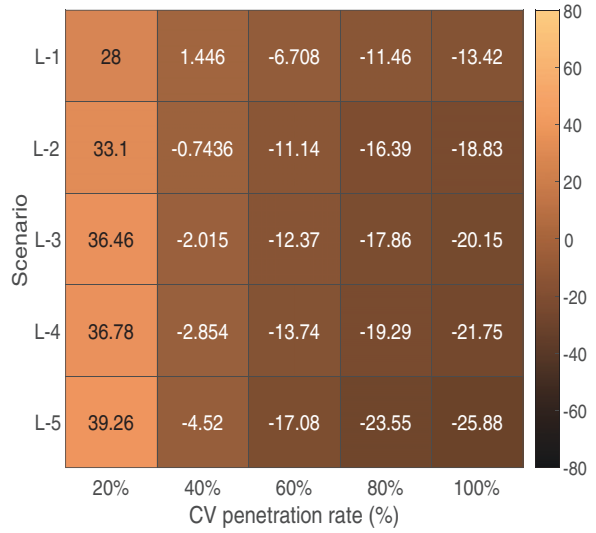


(a) Low traffic demand

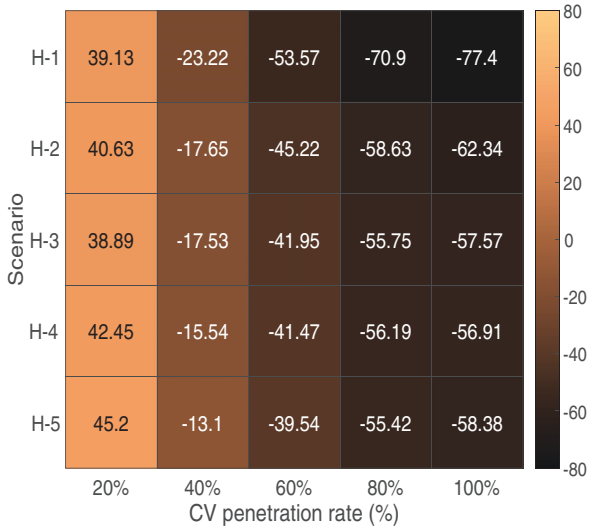


(b) High traffic demand

**FIGURE 13** Difference in average user delay (s) between FAC and UBSTO for different CV penetration rates

the intersection. However, in order to show effectiveness of the proposed strategy also in the case of a penetration rate of CV lower than 100%, we investigate here the performance of the UBSTO when not all vehicles are connected, namely, when the prediction model utilises speed and position from a fraction of vehicles. In this condition, the controller uses only CV data and stop-bar passage times are calculated only for CVs. In particular, we present comparisons with FAC, which is run in its standard way, that is, loop detectors identify all vehicles, irrespective if they are connected or not.The objective of this comparison is to test the controller robustness in a partially CV environment, while unequipped vehicles are not detected and, consequently, not considered in signal timing optimization. Figure 13 illustrates differences in average user delay between UBSTO and FAC for five CV penetration rates between 20% and 100%, for the ten scenarios previously defined. Overall, for CV penetration rate bigger than 40%, UBSTO outperforms FAC for all arrival profiles. A notable point in comparison between low and high traffic scenarios is a contradictory trend that appears by increasing user arrivals. In low traffic demand, increasing the average number of arrival users and the ratio of arrival users of major approaches to minor approaches lead to a decrease in user delay; while in the high traffic we witness the opposite. This difference is attributed to the nature of the UBSTO, where the controller maximises user throughput. The UBSTO strategy can serve a higher number of users by providing a longer green time duration to minor approaches in low user arrival scenarios and a longer green time to major approaches in high user arrival scenarios. As the traffic flow is low, excess delay is not generated in the opposite phase while in the high traffic demand serving higher vehicles from major approaches causes long queues on minor approaches as there are mainly U1 and U2 in high user arrival scenarios. This contradiction is not observed in the difference in term of user throughput between UBSTO and FAC according to Figure 14. Similarly to delay, UBSTO outperforms actuated controller for penetration rate between 40% and 100% in terms of throughput. However, greater changes can be seen in high user arrival scenarios for both low and high traffic condition.

In addition to user-related performance measures, it is relevant to evaluate some vehicle-related performance measures that have an indirect influence on users, such as fuel consumption and emissions. Accordingly, we examine here the average number of stops per vehicle as a proxy indicator of fuel consumption and emissions [74]. In Figure 15, we show the average number of stops per vehicle for the UBSTO strategy in different CV penetration rates compared to FAC in low and high traffic demand. For both traffic conditions, the average number of stops per vehicle obtained with UBSTO is smaller than the one obtained with FAC for CV penetration rates larger than 60%. However, in low traffic conditions, FAC has better performance than UBSTO from 40% penetration rate; whereas in high traffic conditions, UBSTO outperforms FAC for penetration rates lower than 40%.

## 4.5 | Impact of cycle dynamic adaptation in different CV penetration rates

The UBSTO strategy can be applied without the cycle adaption module, namely just implementing the results obtained from the optimisation problem. As previously explained, this is expected to cause extra delay time due to the fact that throughput-maximising optimum green times that satisfy the constraints may still result in an excess of green time at the end of each phase. This is expected to be more evident in low traffic conditions. Moreover, it is relevant to investigate the impact of such module in the case of lower penetration rate, where only a subset of vehicles approaching the intersection are detected.

We compare average performance of 20 random seeds in user demand combination 3 for low and high traffic condition (L-3 and H-3), where we measure average user delay and throughput with cycle adaption module, without cycle adaptation module,

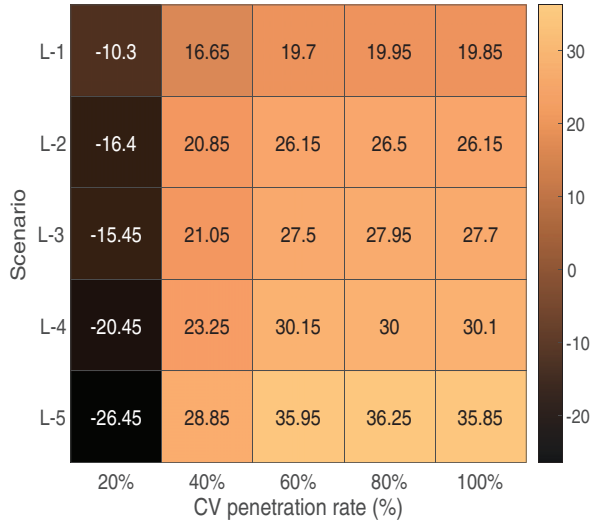


(a) Low traffic demand

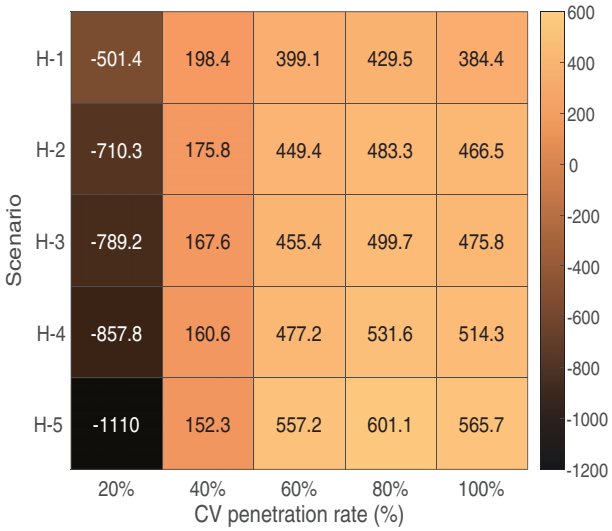


(b) High traffic demand

**FIGURE 14** Difference in user throughput between FAC and UBSTO for different CVs penetration rates

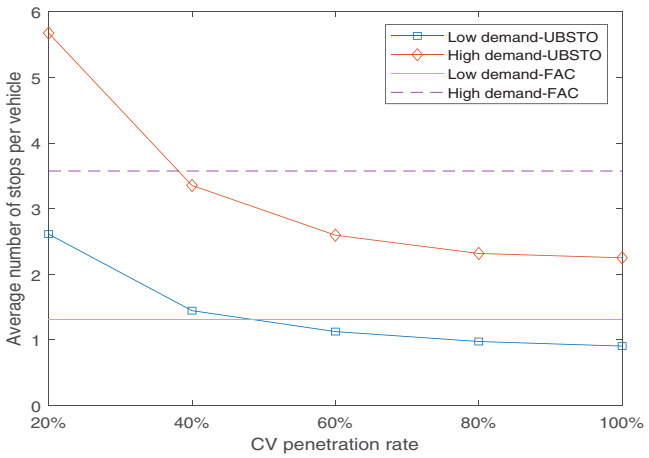


**FIGURE 15** Comparison of average number of stops per vehicles in UBSTO and FAC

both for CV penetration rates between 20% and 100%, comparing them also to FAC.

We illustrate the comparison results in Figure 16, which reveals that applying the cycle adaptation module results in lower delay for CV penetration rate higher than 40%, whereas for smaller penetration rate, the strategy without this module leads to better performance. The adverse performance of the cycle adaptation module in low penetration rate is attributed to the fact that the module cuts the excess green time based on the last detected vehicle's predicted arrival time, which may actually not be the last vehicle capable to cross the intersection. In such case, such non-connected vehicles are forced to stop until the next cycle, increasing the average delay. Conversely, when the strategy is run without the module, excess green times may facilitate serving unequipped vehicles. Additionally, user throughput analysis shows that applying the cycle adaptation module in high traffic condition generates improved performance compared to not applying the module. However, in low traffic condition, applying the module causes adverse performance for penetration rates lower than 60%.

## 5 | CONCLUSIONS

### 5.1 | Results summary and discussion

The merit of this research lies in the development of a traffic control strategy aimed at finding the optimum signal timing that maximises user throughput within a signal cycle, using CV data. Our strategy consists of three main components which are user throughput prediction, signal timing optimisation and cycle dynamic adaptation. Considering the features of the modules, the strategy maximises user throughput while adapting the cycle length and split times to user arrival and traffic conditions. We tested intersection performance for five distinct user demand combinations and two vehicular traffic conditions using experiments on a synthetic intersection in a microscopic traffic simulator. The efficiency of proposed strategy has been compared to the state-of-the-art actuated signal control. The user throughput and average user delay have been measured for each of the mentioned conditions. In addition, as a proxy measurement for fuel consumption and emission, we also measured UBSTO's ability in decreasing the number of stops per vehicle.

To the best of our knowledge, maximising user throughput using an adaptive controller in a CV environment has not been investigated in previous research, as most of the research is focused on vehicle-centred strategies. Additionally, in contrast with previous works, we consider different passenger vehicle classes based on number of users on-board, as opposed to assuming the same occupancy for all passenger vehicles. The presented results show efficiency of UBSTO in controlling the signal timing. In general, the results show that the proposed strategy considerably improves user-related indicators as well as provides equitable serving of vehicles based on number of users on-board. These improvements are higher during high traffic demand levels. For instance, in a fully connected environment, the user throughput by UBSTO can be around 560 users per

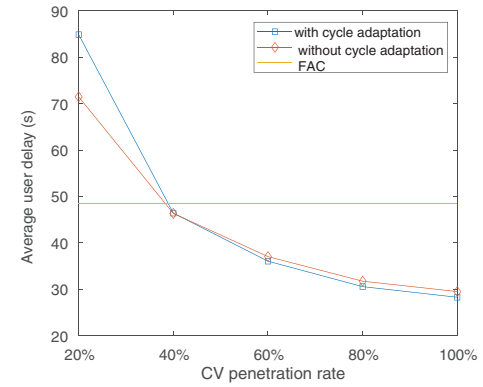


(a) Average user delay-Low traffic condition

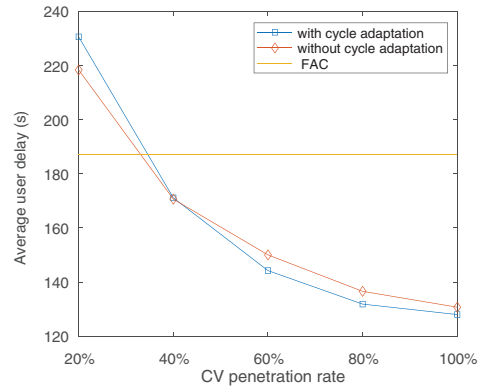


(b) Average user delay-High traffic condition

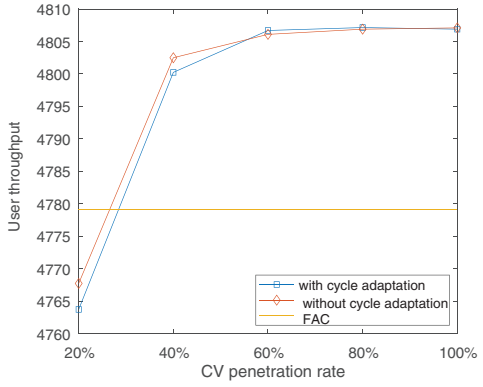


(c) User throughput-Low traffic condition

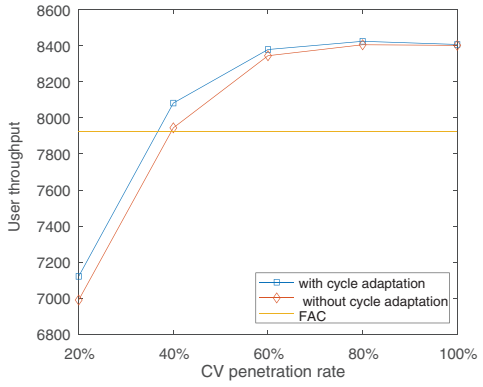


(d) User throughput-High traffic condition

**FIGURE 16** Difference in average user delay between FAC and UBSTO with cycle adaption and without cycle adaption in different CV penetration rates

hour higher for high traffic demand, and 35 users per hour higher in low traffic demand than conventional control. Also, UBSTO can reduce average user delay for around 60 s and 25 s in high and low traffic demand, respectively. Thus, these simulation results show potential of UBSTO to increase user throughput and to decrease user delay.

We measured controller robustness in a partially CV environment when there are unequipped vehicles in the traffic flow. Our proposed control strategy outperforms conventional actuated controller for 40% and higher CV penetration rates. Thus, results show that UBSTO can outperform a conventional fully actuated controller even in low CV penetration rate. These findings have similar trend of impacts in comparison to previous research in traffic signal control that is comparing novel strategies to actuated signal control, for example, [16, 40, 50]. However, most of this previous research does not focus on user-based performance indicators, such as user delay or user throughput, as opposed to UBSTO. Consequently, given the unique experimental setting, direct quantitative comparison using statistical methods is not feasible at the moment.

Besides the potential improvements in traffic operations efficiency, as UBSTO provides priority for vehicles with higher users on-board in comparison with a vehicle-based controller, this can be a supporting mechanism for mobility management strategies. Thus, implementing user-based signal control strategies does not solely serve prioritising the right-of-way for high-occupancy and ride-sharing vehicles, but may also play an important role in supporting behavioral shift to shared mobility services. For example, according to the Federal Highway Administration, the 2018 average vehicles occupancy rate in the US was 1.7 [75] . The same amount is reported according to a survey in the EU [70]. This means that more than 50% capacity of daily private traffic flow is not utilised in most parts of the world, assuming four passengers as vehicle capacity. In fact, low vehicle occupancy is directly related to concerns about energy consumption and emissions, especially with the advancement of automated vehicle technology [76]. On the contrary, we know that special treatment of high-occupancy vehicles in traffic management strategies can affect users' willingness to share their rides [77]. Therefore, there is a clear need to keep on developing and implement user-based strategies in traffic management, if they are to support other sets of sustainable mobility management measures.

Implementation of user-supportive strategies such as UBSTO in practice depends on development of data collection, communication, and controller tools. Firstly, UBSTO needs number of user on-board of each vehicle in addition to vehicle data, however current development of CVs focuses mainly on vehicle-related data. For this purpose, using existing in-vehicle sensor such as seat belt and weighting sensors can be used to collect user data. Secondly, UBSTO needs real-time data as well as other real-time signal timing strategies. In our proposed algorithm, we assumed that optimisation is completed when the closest detected vehicle arrives at the stop-bar. Accordingly, the information needs to be received by the controller in advance and detection range depend on communication speed and

controller processor power. Limitation of conventional data collection tools might be the main reason of limited attention to users in signal timing strategies, but novel technologies such as CV can provide sufficient data to implement user-based signal timing. In this research, we assumed that number of users on each vehicle is available as well as other vehicle-related such as speed and position. However, vehicles data are the critical data for our algorithm. Thus, UBSTO can work when the number of user of a vehicle is missing but vehicle data is available. To achieve this, we can assume the number of users in each vehicle based on, for example, statistical data [78]. Alternatively, in the case of missing data for the number of users, our strategy can be switched to just vehicle-based mode which maximises vehicle throughput. The proper performance of VBSTO has been also illustrated by the above results. In either case, the experimental setup established in this research has aimed at following the best practice of simulation-based evaluation. Demand patterns used for the case intersection, including intersection layout, are in line with similar research, for example, [4, 7, 43] and general signal timing guidelines [79].

## 5.2 | Future development

This development opens up several pathways for future research. First, UBSTO strategy should be implemented on road networks with additional transport modes, such as buses, bicycles and pedestrians. For this implementation, one can rely on either case study measurements or empirically-generated demand distributions. In these scenarios, UBSTO strategy can be further developed to account for deviation from the schedule of public transport vehicles in addition to the number of users on-board, or special weight assigned to travel time for cyclists and pedestrians - if these modes are to be prioritised further. Second, the stop-bar passage time prediction model has been developed for a CV environment. In future research, stop-bar passage time prediction can be extended to a mixed traffic condition while there are unequipped vehicles in the traffic flow. In this condition, it is necessary to design an estimation algorithm capable of providing the necessary information on unequipped vehicles by using available information from CVs. Third, the UBSTO strategy could be tested on networks with multiple adjacent intersections. In this case, the spillback effect in oversaturated conditions has to considered. Such evaluation should include expanded set of performance measures for such cases, for example, queue lengths and direct emissions, in order to evaluate performance at intersection and network level. This research pathway certainly leads to asking higher level questions of the selection of performance measures used for evaluating of new CV-based control strategies, especially in relation to existing actuated control. Fourth, considering lessons from development and deployment of traffic responsive and adaptive control systems around the world, there is a further need to evaluate thresholds and trigger conditions for switching between traffic control strategies that will rely on conventional and CV detection technology. Those control actions are especially important to evaluate if penetration rates keep on varying over time, such as during a day or week. Fifth, in addition to vehicle-to-infrastructure connectivity, vehicle-to-vehicle communication, driving assistance systems, and automation are expected to provide significant opportunities for traffic management, with potential benefits to traffic flow; see, for example, [26, 80–82]. Although in this work we focus on manually-driven vehicles, the method can be modified and improved by considering automated vehicles capabilities.

## ACKNOWLEDGEMENT

This research is partly funded by the Henry Ford Foundation Finland and the FINEST Twins Center of Excellence (H2020 European Union funding for Research & Innovation grant 856602).

## ORCID

*Roozbeh Mohammadi* https://orcid.org/0000-0003-1290-4499
*Claudio Roncoli* https://orcid.org/0000-0002-9381-3021
*Miloš N. Mladenović* https://orcid.org/0000-0002-3746-3573

## REFERENCES

1. Papageorgiou, M., et al.: Review of road traffic control strategies. Proc. IEEE 91(12), 2043–2067 (2003)
2. Mladenovic, M.: Large scale analysis of traffic control systems. Traffic Eng. Control 53(1), 26–32 (2012)
3. Hamilton, A., et al.: The evolution of urban traffic control: Changing policy and technology. Transport. Plan. Technol. 36(1), 24–43 (2013)
4. Mirheli, A., et al.: Development of a signal-head-free intersection control logic in a fully connected and autonomous vehicle environment. Transport. Res. Part C: Emerg. Technol. 92, 412–425 (2018)
5. Sun, X., Yin, Y.: A simulation study on max pressure control of signalized intersections. Transp. Res. Rec. 2672(18), 117–127 (2018)
6. Mohajerpoor, R., et al.: Analytical derivation of the optimal traffic signal timing: Minimizing delay variability and spillback probability for undersaturated intersections. Transport. Res. Part B: Methodolog. 119, 45–68 (2019)
7. Liang, X.J., et al.: A heuristic method to optimize generic signal phasing and timing plans at signalized intersections using connected vehicle technology. Transport. Res. Part C: Emerg. Technol. 111, 156–170 (2020)
8. Bonneson, J.A., Abbas, M.: Intersection Video Detection Field Handbook. Technical Report. Texas Transportation Institute, Texas A & M University System, Texas (2002)
9. Klein, L.A., et al.: Traffic Detector Handbook, 3rd edn., Vol. ii. Technical Report No. FHWA-HRT-06-139. Federal Highway Administration, Washington, DC (2006)
10. Klein, L.A., et al.: Traffic Detector Handbook, 3rd edn., Vol. i. Technical Report No. FHWA-HRT-06-108. Federal Highway Administration, Washington, DC (2006)
11. Baker, R.J., et al.: An overview of transit signal priority. Technical Report. ITS America, Washington DC (2002)
12. Dion, F., et al.: Evaluation of potential transit signal priority benefits along a fixed-time signalized arterial. J. Transp. Eng. 130(3), 294–303 (2004)
13. Smith, H.R., et al.: Transit Signal Priority (TSP): A Planning and Implementation Handbook. ITS America, DOT, Washington, DC (2005)
14. Qin, X., Khan, A.M.: Control strategies of traffic signal timing transition for emergency vehicle preemption. Transport. Res. Part C: Emerg. Technol. 25, 1–17 (2012)
15. Hannoun, G.J., et al.: Facilitating emergency response vehicles' movement through a road segment in a connected vehicle environment. IEEE Trans. Intell. Transp. Syst. 20(9), 3546–3557 (2018)
16. Li, Z., et al.: Signal control optimization for automated vehicles at isolated signalized intersections. Transport. Res. Part C: Emerg. Technol. 49, 1–18 (2014)

17. Mohan, M., Chandra, S.: Queue clearance rate method for estimating passenger car equivalents at signalized intersections. J. Traffic Transport. Eng. 4(5), 487–495 (2017)
18. De Nunzio, G., et al.: Speed advisory and signal offsets control for arterial bandwidth maximization and energy consumption reduction. IEEE Trans. Control Syst. Technol. 25(3), 875–887 (2017)
19. Zhou, Z., et al.: Two-level hierarchical model-based predictive control for large-scale urban traffic networks. IEEE Trans. Control Syst. Technol. 25, 496–508 (2017)
20. Geroliminis, N., et al.: A three-dimensional macroscopic fundamental diagram for mixed bi-modal urban networks. Transport. Res. Part C: Emerg. Technol. 42, 168–181 (2014)
21. Chiabaut, N.: Evaluation of a multimodal urban arterial: The passenger macroscopic fundamental diagram. Transport. Res. Part B: Methodolog. 81, 410–420 (2015)
22. Jacobson, J., Sheffi, Y.: Analytical model of traffic delays under bus signal preemption: theory and application. Transport. Res. Part B: Methodological 15(2), 127–138 (1981)
23. Mahmassani, H.S.: 50th anniversary invited article—Autonomous vehicles and connected vehicle systems: Flow and operations considerations. Transport. Sci. 50(4), 1140–1162 (2016)
24. Guo, Q., et al.: Urban traffic signal control with connected and automated vehicles: A survey. Transportation research part C: emerging technologies 101, 313–334 (2019)
25. Guler, S.I., et al.: Using connected vehicle technology to improve the efficiency of intersections. Transport. Res. Part C: Emerg. Technol. 46, 121–131 (2014)
26. Yang, K., et al.: Isolated intersection control for various levels of vehicle technology: Conventional, connected, and automated vehicles. Transport. Res. Part C: Emerg. Technol. 72, 109–129 (2016)
27. Yang, K., et al.: Multi-scale perimeter control approach in a connected-vehicle environment. Transp. Res. Procedia 23, 101–120 (2017)
28. Jung, R., Gan, A.: Sampling and analysis methods for estimation of average vehicle occupancies. J. Transp. Eng. 137(8), 537–546 (2010)
29. Jung, R., et al.: Vehicle occupancy data collection methods. Technical Report No. BD-015-9. Florida International University, State of Florida Department of Transportation, Florida (2005)
30. Mladenović, M.N., et al.: Development of socially sustainable traffic-control principles for self-driving vehicles: The ethics of anthropocentric design. In: Proceedings of the IEEE 2014 International Symposium on Ethics in Engineering, Science, and Technology, p. 77. IEEE, Piscataway (2014)
31. Li, L., et al.: A survey of traffic control with vehicular communications. IEEE Trans. Intell. Transp. Syst. 15(1), 425–432 (2014)
32. Jiang, H., et al.: Eco approaching at an isolated signalized intersection under partially connected and automated vehicles environment. Transport. Res. Part C: Emerg. Technol. 79, 290–307 (2017)
33. Xu, B., et al.: Cooperative method of traffic signal optimization and speed control of connected vehicles at isolated intersections. IEEE Trans. Intell. Transp. Syst. 99, 1–14 (2018)
34. Bichiou, Y., Rakha, H.A.: Developing an optimal intersection control system for automated connected vehicles. IEEE Trans. Intell. Transp. Syst. 20, 1908–1916 (2019)
35. Rafter, C.B., et al.: Augmenting traffic signal control systems for urban road networks with connected vehicles. IEEE Trans. Intell. Transp. Syst. 21(4), 1728–1740 (2020)
36. Mohammadi, R., et al.: Transit signal priority in a connected vehicle environment: User throughput and schedule delay optimization approach. In: 2020 Forum on Integrated and Sustainable Transportation Systems (FISTS), pp. 252–257. IEEE, Piscataway (2020)
37. Hu, J., et al.: Transit signal priority with connected vehicle technology. Transp. Res. Rec. 2418(1), 20–29 (2014)
38. Hu, J., et al.: Coordinated transit signal priority supporting transit progression under connected vehicle technology. Transport. Res. Part C: Emerg. Technol. 55, 393–408 (2015)
39. Hu, J., et al.: Transit signal priority accommodating conflicting requests under connected vehicles technology. Transport. Res. Part C: Emerg. Technol. 69, 173–192 (2016)
40. He, Q., et al.: Multi-modal traffic signal control with priority, signal actuation and coordination. Transport. Res. part C: Emerg. Technol. 46, 65–82 (2014)
41. Wu, W., et al.: Integrated optimization of bus priority operations in connected vehicle environment. J. Adv. Transp. 50(8), 1853–1869 (2016)
42. Beak, B., et al.: Peer-to-peer priority signal control strategy in a connected vehicle environment. Transp. Res. Rec. 2672(18), 15–26 (2018)
43. Yang, K., et al.: Implementing transit signal priority in a connected vehicle environment with and without bus stops. Transportmetrica B: Transport Dyn. 7(1), 423–445 (2019)
44. Wu, K., Guler, S.I.: Estimating the impacts of transit signal priority on intersection operations: A moving bottleneck approach. Transport. Res. Part C: Emerg. Technol. 105, 346–358 (2019)
45. Teng, K., et al.: Transit priority signal control scheme considering the coordinated phase for single-ring sequential phasing under connected vehicle environment. IEEE Access 7, 61057–61069 (2019)
46. Abdelhalim, A., Abbas, M.: Impact assessment of a cooperative bus-holding transit signal priority strategy. In: 2018 21st International Conference on Intelligent Transportation Systems (ITSC), pp. 1908–1913. IEEE, Piscataway (2018)
47. Christofa, E., Skabardonis, A.: Traffic signal optimization with application of transit signal priority to an isolated intersection. Transp. Res. Rec. 2259(1), 192–201 (2011)
48. Christofa, E., et al.: Person-based traffic signal optimization for real-time applications. In: Transportation Research Board 91st Annual Meeting (12-2228). Transportation Research Board, Washington DC (2012)
49. Christofa, E., et al.: Person-based traffic responsive signal control optimization. IEEE Trans. Intell. Transp. Syst. 14(3), 1278–1289 (2013)
50. Christofa, E., et al.: Arterial traffic signal optimization: A person-based approach. Transport. Res. Part C: Emerg. Technol. 66, 27–47 (2016)
51. Yu, Z., et al.: Person-based optimization of signal timing: Accounting for flexible cycle lengths and uncertain transit vehicle arrival times. Transp. Res. Rec. (2620), 31–42 (2017)
52. Yu, Z., et al.: Implementing phase rotation in a person-based signal timing optimization framework. In: 2018 21st International Conference on Intelligent Transportation Systems (ITSC), pp. 20–25. IEEE, Piscataway (2018)
53. Farid, Y.Z., et al.: An analytical model to conduct a person-based evaluation of transit preferential treatments on signalized arterials. Transport. Res. Part C: Emerg. Technol. 90, 411–432 (2018)
54. Zeng, X., et al.: Person-based adaptive priority signal control with connected-vehicle information. Transp. Res. Rec. 2487(1), 78–87 (2015)
55. Chou, L.-D., et al.: A passenger-based adaptive traffic signal control mechanism in intelligent transportation systems. In: 2012 12th International Conference on ITS Telecommunications, pp. 408–411. IEEE, Piscataway (2012)
56. Ma, W., et al.: Integrated optimization of transit priority operation at isolated intersections: A person-capacity-based approach. Transport. Res. Part C: Emerg. Technol. 40, 49–62 (2014)
57. Yang, H., et al.: Eco-cooperative adaptive cruise control at signalized intersections considering queue effects. IEEE Trans. Intell. Transp. Syst. 18(6), 1575–1585 (2017)
58. Liu, H., et al.: Traffic signal control by leveraging cooperative adaptive cruise control (CACC) vehicle platooning capabilities. Transport. Res. Part C: Emerg. Technol. 104, 390–407 (2019)
59. Mohammadi, R., et al.: User throughput optimization for signalized intersection in a connected vehicle environment. In: 2019 6th International Conference on Models and Technologies for Intelligent Transportation Systems (MT-ITS). IEEE, Piscataway (2019)
60. Feng, Y., et al.: Spatiotemporal intersection control in a connected and automated vehicle environment. Transport. Res. Part C: Emerg. Technol. 89, 364–383 (2018)
61. Feng, Y., et al.: A real-time adaptive signal control in a connected vehicle environment. Transport. Res. Part C: Emerg. Technol. 55, 460–473 (2015)
62. Lighthill, M.J., Whitham, G.B.: On kinematic waves ii. A theory of traffic flow on long crowded roads. Proc. R. Soc. London, Ser. A. Math. Phys. Sci. 229(1178), 317–345 (1955)

63. Talebpour, A., Mahmassani, H.S.: Influence of connected and autonomous vehicles on traffic flow stability and throughput. Transport. Res. Part C: Emerg. Technol. 71, 143–163 (2016)
64. Mukherjee, D., Mitra, S.: A comparative study of safe and unsafe signalized intersections from the view point of pedestrian behavior and perception. Accid. Anal. Prev. 132, 105218 (2019)
65. Yun, M., et al.: Lane change behavior at weaving section of signalized intersection upstream. In: ICTE 2013: Safety, Speediness, Intelligence, Low-Carbon, Innovation, pp. 1229–1234. American Society of Civil Engineers, Reston (2013)
66. Wang, J., et al.: Multi-objective optimal cooperative driving for connected and automated vehicles at non-signalised intersection. IET Intel. Transport Syst. 13(1), 79–89 (2019)
67. Ceylan, H., Bell, M.G.: Traffic signal timing optimisation based on genetic algorithm approach, including drivers' routing. Transport. Res. Part B: Methodol. 38(4), 329–342 (2004)
68. Li, Z., et al.: Intersection control optimization for automated vehicles using genetic algorithm. J. Transp. Eng., Part A: Systems 144(12), 04018074, (2018)
69. Koonce, P., Rodegerdts, L.: Traffic Signal Timing Manual. Technical Report No. FHWA-HOP-08-024. U.S. Department of Transportation, Washington DC (2008)
70. Fiorello, D., et al.: Mobility data across the eu 28 member states: Results from an extensive cawi survey. Transp. Res. Procedia 14, 1104–1113 (2016)
71. PTV Vissim, 11.00-03 User Manual (2018).
72. PTV America, Ring Barrier Controller User Manual (2010).
73. PTV Vistro, 5.00-05 User Manual (2017).
74. Rakha, H., Ding, Y.: Impact of stops on vehicle fuel consumption and emissions. J. Transp. Eng. 129(1), 23–32 (2003)
75. Administration, F.H.: Average vehicle occupancy factors for computing travel time reliability measures and total peak hour excessive delay metrics. Technical Report. Federal Highway Administration (FHWA), Washington DC (2018)
76. Soteropoulos, A., et al.: Impacts of automated vehicles on travel behaviour and land use: An international review of modelling studies. Transport Rev. 39(1), 29–49 (2019)
77. Neoh, J.G., et al.: What encourages people to carpool? An evaluation of factors with meta-analysis. Transportation 44(2), 423–447 (2017)
78. Levine, N., Wachs, M.: Factors affecting vehicle occupancy measurement. Transport. Res. Part A: Policy Pract. 32(3), 215–229 (1998)
79. Urbanik, T., et al.: Signal Timing Manual, 2ndedn. Transportation Research Board, Washington DC (2015).
80. Guo, Y., et al.: Joint optimization of vehicle trajectories and intersection controllers with connected automated vehicles: Combined dynamic programming and shooting heuristic approach. Transport. Res. Part C: Emerg. Technol. 98, 54–72 (2019)
81. Liang, X.J., et al.: Joint optimization of signal phasing and timing and vehicle speed guidance in a connected and autonomous vehicle environment. Transp. Res. Rec. 2673(4), 70–83 (2019)
82. Tajalli, M., et al.: Network-level coordinated speed optimization and traffic light control for connected and automated vehicles. IEEE Trans. Intell. Transp. Syst. (2020)

**How to cite this article:** Mohammadi R, Roncoli C, Mladenović MN. Signalised intersection control in a connected vehicle environment: User throughput maximisation strategy. *IET Intell Transp Syst*. 2021;1–20. https://doi.org/10.1049/itr2.12038